Ten-vertex Metallaborane Chemistry. Aspects of the Iridadecaborane *closo→isonido→isocloso* Structural Continuum†

Jonathan Bould, John D. Kennedy* and Mark Thornton-Pett
School of Chemistry, University of Leeds, Leeds LS2 9JT, UK

Reaction of the *arachno*-$[B_9H_{14}]^-$ or *nido*-$[B_9H_{12}]^-$ anions with $[IrCl(PPh_3)_3]$ at *ca.* 298 K gives, in addition to previously reported species, pale violet $[7,7,9\text{-}(PPh_3)_3\text{-}isonido\text{-}7\text{-}IrB_9H_{10}]$ **2** in yields of *ca.* 2%. Single crystal X-ray diffraction analysis and multinuclear NMR spectroscopy reveal a ten-vertex $\{IrB_9\}$ cluster of an '*isonido*' type that is based upon the *closo* eleven-vertex structure of $[B_{11}H_{11}]^{2-}$ from which a four-connected vertex is removed to generate a four-membered open face. There are two fluxional bridging hydrogen atoms associated with the open face. Thermolysis at *ca.* 355 K of solutions in 1,1,2,2-tetrachloroethane of yellow $[5,7\text{-}(PPh_3)_2\text{-}5\text{-}H\text{-}5\text{-}(o\text{-}Ph_2PC_6H_4)\text{-}nido\text{-}5\text{-}IrB_9H_{10}\text{-}2]$ **4** result in loss of hydrogen and the formation of deep purple $[8\text{-}Cl\text{-}7,9\text{-}(PPh_3)_2\text{-}7\text{-}(o\text{-}Ph_2PC_6H_4)\text{-}isonido\text{-}7\text{-}IrB_9H_6\text{-}10]$ **5** (0–5%) and royal blue $[7,9\text{-}(PPh_3)_2\text{-}7\text{-}(o\text{-}Ph_2PC_6H_4)\text{-}isonido\text{-}7\text{-}IrB_9H_9\text{-}10]$ **6** (0–5%). Single-crystal X-ray diffraction shows that compounds **5** and **6** also have *isonido* cluster structures, although **5** does not have bridging hydrogen atoms on the open face, suggesting that any extra electrons required for it to be isoelectronic with **2** and **6** may originate from the metal vertex. The structure of the crystal of compound **6** examined was found to contain *ca.* 25 mole % of the isostructural 3-chloro derivative **6a**. The ten-vertex clusters **2**, **5** and **6** are part of a structural continuum ranging from *closo* through *isonido* to *isocloso*. It is proposed that these *isonido* compounds represent intermediates in a variety of reactions involving *nido* to *isocloso* cluster oxidations and *nido* to *nido* rearrangements.

The systematisation of chemical observations into related patterns is one of the steps by which the classification of compounds and reactions can be initiated, and it is thereby one of the important steps by which science develops. Two elements that are adjacent in the first row of the Periodic Table, boron and carbon, are unique in forming extensive series of complex hydrides. The patterns of structure and reactivity of the carbon hydrides are of course well systematised and recognised, and they constitute one of the fundamental bases of the subdiscipline that is known as organic chemistry. The boron hydrides or boranes, which typically adopt polyhedral cage or cluster structures, are less generally familiar. The establishment of the systematics of the *reaction* chemistry of the boranes and their heteroanalogues continues to be one of the challenges of contemporary Inorganic Chemistry. By contrast, the basic patterns governing the observable *structures* of the basic polyhedral boranes and related species were recognised and classified some twenty years ago by Williams and Wade.[1,2] They have played a dominant role in the development of the extensive chemistry of these species.

For the further development of this chemistry there is some importance in recognising, describing and delineating observed *systematic* deviations from these initial structural patterns.[3] In this context we here describe and discuss examples constituting a new systematic structural pattern in ten-vertex boron-containing cluster chemistry.

Using the nomenclature of the accepted categorisation [1,2] in boron-containing cluster chemistry, the classical ten-vertex *closo* structure is that of an Archimedian bicapped square antiprism (structure **I**) of D_{4d} symmetry. The classical ten-vertex *nido* structure has the boat-shaped C_{2v} geometry as in structure **II**. According to the recognised patterns, this is geometrically derived from the *closo* eleven-vertex closed C_{2v} structure by removal of the vertex of highest connectivity (structure **III**), thus generating the open cluster which has a six-membered open face.

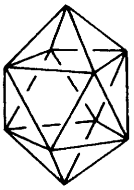
I

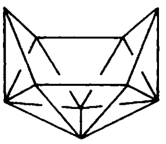
II

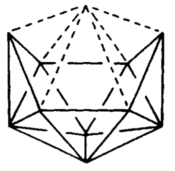
III

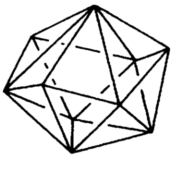
IV

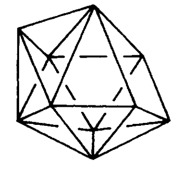
V

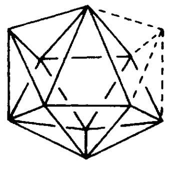
VI

Since the original Williams–Wade classifications,[1,2] an alternative closed structure **IV** has been recognised in a number of metallaboranes and related species.[4,5] This is of three-fold C_{3v} symmetry and has been given the descriptor *isocloso*. An alternative open structure **V** can also occur.[5–7] This last structure is derived geometrically from the *closo* eleven-vertex closed C_{2v} structure by removal of a vertex of cluster connectivity four (structure **VI**), and has been given the descriptor *isonido*. It has a four-membered open face. This ten-vertex *isonido* structure has been invoked, but not observed, in a variety of metallaborane and related systems.[4,5,8,9]

It can be seen that there is a continuum of structure between the classical *closo* and the *isocloso* ten-vertex metallaborane structures (Scheme 1). The structures are interconverted through a diamond–square–diamond[10] rearrangement *via* an open face which passes through the *isonido* geometry.

---

† *Supplementary data available:* see Instructions for Authors, *J. Chem. Soc., Dalton Trans.*, 1992, Issue 1, pp. xx–xxv.

Non-SI unit employed: eV ≈ 1.60×10^{-19} J

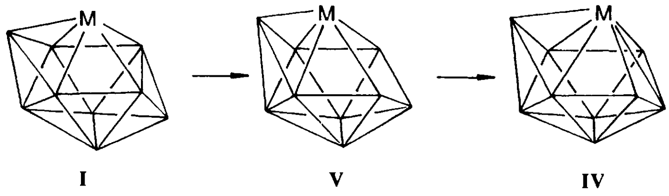

I V IV

Scheme 1

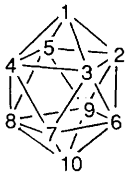

VII

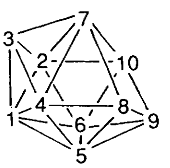

VIII

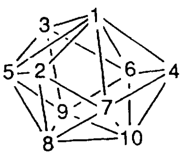

IX

The *isocloso* cluster structure **IV** is now well documented, and we have recently described some ten-vertex *isocloso*-1-iridadecaboranes typified by $[(PPh_3)(Ph_2PC_6H_4)HIrB_9H_8]$.[4] By contrast, *isonido* ten-vertex compounds of structure **V** are as yet sparsely documented.[5-7] Here we report on a series of *isonido* iridaboranes of schematic cluster type **V**. We have found it very difficult reproducibly to obtain viable quantities of pure samples of some of these materials for complete intercomparative characterisation. This has particularly hindered the matching of NMR spectra with some of the results of single-crystal diffraction work. Aspects of the overall work are therefore not yet as defined as we would wish. Nevertheless there is value in reporting what we have been able to determine so far, in view both of the novelty of the structures and of the theoretical interest in this and closely related areas.[8,11-14]

Some related[4,15] work has been reported previously, and aspects of the work have been mentioned in review articles.[4,5,16,17] The original example of an *isonido* species, the purple iridacarbaborane $[(PPh_3)(Ph_2PC_6H_4)IrB_8H_6(OMe)C(OH)]$ (compound **8**) was reported in a preliminary note some time ago.[6] Very recently the structure of a second low-yield compound, *viz* red $[3\text{-}(OEt)\text{-}4,9\text{-}(PPh_3)_2\text{-}7\text{-}Cl\text{-}7\text{-}(o\text{-}Ph_2PC_6H_4)\text{-}isonido\text{-}7\text{-}IrB_9H_5\text{-}8]$ **7**, has also been reported.[7]

The numbering schemes for the ten-vertex *closo*, *isonido*, and *isocloso* clusters encountered in this paper are given in structures **VII**, **VIII** and **IX** respectively.

Results and Discussion

Preparation and Characterisation of Compounds.—The reaction between $[IrCl(PPh_3)_3]$ and *arachno*-$[B_9H_{14}]^-$ in dichloromethane solution at ambient temperature gives *ca.* 80% yields of the previously described[8,18] yellow *nido*-6-iridadecaborane compound $[H(PPh_3)_2IrB_9H_{13}]$ **1**, plus variable yields of up to *ca.* 2% of a pale violet compound **2**. This violet species **2** is similarly often produced in a small but variable yield, together with a number of bright yellow *nido*-5- and -6-iridadecaborane cluster species,[8] when the borane anion used is *nido*-$[B_9H_{12}]^-$. Here we now describe the characterisation of compound **2** by single-crystal X-ray diffraction analysis, and multielement NMR and infrared spectroscopies, as $[7,7,9\text{-}(PPh_3)_3\text{-}isonido\text{-}7\text{-}IrB_9H_{10}]$.

An ORTEP diagram of the molecular structure is shown in Fig. 1. Tables 1 and 2 list selected values for interatomic separations and angles. All heavy atoms and the eight cluster *exo*-terminal hydrogen atoms were located in the diffraction analysis, and ^1H NMR spectroscopy (Table 3) showed that there were two additional cluster-bound hydrogen atoms, presumably bridging and associated with the open face, which were not locatable directly from the diffraction data. The proposed positions of these hydrogen atoms (Fig. 1) were derived from a consideration of other factors (next paragraphs).

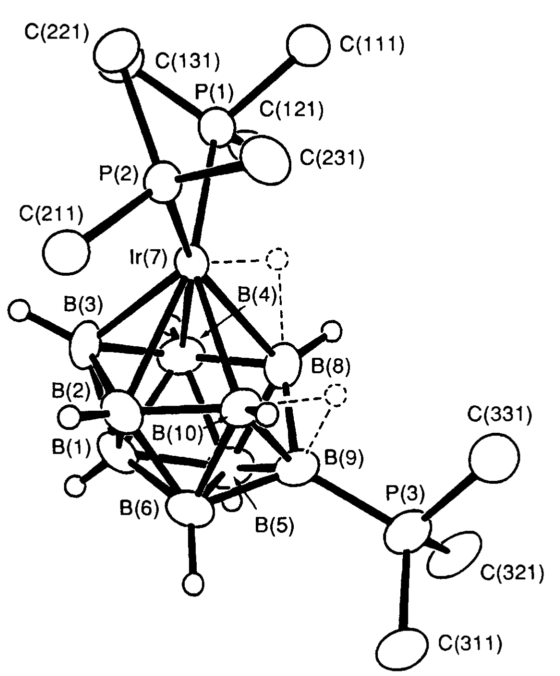

Fig. 1 ORTEP drawing of $[7,7,9\text{-}(PPh_3)_3\text{-}isonido\text{-}7\text{-}IrB_9H_{10}]$ **2** with P-phenyl group atoms (except for the *ipso* carbon ones) omitted for clarity. All atoms were located with the exception of the two bridging hydrogen atoms associated with the open face of the cluster. The proposed positions of these latter atoms as illustrated (hatched lines) were determined from a consideration of other factors as described in the text

The other NMR data (Table 3) are reasonably in accord with the X-ray structure and show nine boron resonances, eight associated with *exo*-terminal hydrogen atoms and one with an attached PPh_3 ligand $[^2J(^{31}P\text{-}^{11}B)$ 185 Hz].

The precise natures of the bridging hydrogen atoms are difficult to ascertain. The room-temperature proton NMR spectrum reveals a resonance of relative intensity two at $\delta(^1H)$ -6.65, for which $^1H\text{-}\{^{31}P\}$ spectroscopy reveals a small coupling to ^{31}P. On cooling, the resonance broadens, then separates into two components. One of these, at $\delta(^1H)$ -4.37, is in the region usually associated with B–H–B bridging hydrogen atoms, with the other one, at $\delta(^1H)$ -8.70, in the region normally associated with an iridium hydride bridging to boron. The latter resonance also features equivalent coupling to two phosphorus atoms $[^2J(^{31}P\text{-}^1H)$ 18 Hz]. The low-temperature B–H–B resonance does not feature any coupling to atom P(3), but there are few reported comparison examples of couplings to phosphorus of hydrogen atoms bridging to phosphine-substituted boron atoms, and in addition it is known that ^2J couplings to phosphorus can pass through zero.[20] For appropriate metallaborane compounds that have been reported[21,22] the magnitudes of these couplings are small (<7 Hz) or unobserved. It would be useful to have further comparison data in this area. In the 100 MHz spectrum the two proton resonances coalesce at 250 K, yielding a calculated activation energy, $\Delta G^‡_{250}$, of 46.5 kJ mol^{-1} for their exchange. This is in the range found for fluxional processes involving a twist contrarotation of metal-bound phosphine ligands with respect to a borane cage, as in, for example, the η^4-bonded metallaboranes $[(CO)(PMe_3)_2\text{-}arachno\text{-}IrB_4H_9]$[23] (64 kJ mol^{-1}) and $[(PMe_2Ph)_2\text{-}nido\text{-}PtB_{10}H_{12}]$[24] (80 kJ mol^{-1}), the η^5-bonded species $[(PMe_2Ph)_2\text{-}closo\text{-}PtE_2B_9H_{12}]$ (E = As or C)[25] ($<$*ca.* 30 kJ mol^{-1}), and the η^6-bonded species $[(PMe_2Ph)_2PtC_2B_8H_9R]$[26] (R = H, Me or Ph; 30–85 kJ mol^{-1}). In the case of compound **2**, however, we believe that the fluxionality arises from chemical exchange between the two 'bridging' hydrogen atoms, rather than being associated with a gross *exo*-polyhedral ligand-sphere rotational process.

The exact bonding mode of these two hydrogen atoms is difficult to assess further by NMR spectroscopy since the temperatures required to freeze the exchange on the NMR time-scale also result in essentially complete 'thermal' decoupling[27,28] of the signals of this relatively bulky molecule. Thus it was not possible to determine by selective $^1H-\{^{11}B\}$ experiments (*a*) whether the resonance at δ −8.70 is in fact due to a terminal iridium hydride or an Ir–H–B bridging hydrogen atom, or (*b*) with which boron atoms the resonance at δ −4.37 is associated. The chemical shift of δ −8.70 is in the region associated with iridium–boron bridging hydrides in known conventional *nido*-iridadecaboranes [$\delta(^1H)$ usually −5 to −10],[8,18] and is significantly to lower field than the chemical shifts usually found for terminal iridium hydrides in iridaboranes (Table 4). However, the known ten-vertex *closo* iridacarbaborane [1,2,2-$(PPh_3)_3$-2-H-*closo*-2,10-$IrCB_8H_{10}$] **3** features a resonance at $\delta(^1H)$ −4.36 ascribed to a terminal iridium hydride,[30] as does the known eleven-vertex cluster compound [$(PPh_3)_2HIrC_2B_8H_{10}$] [$\delta(^1H)$ −6.26][31] which also has some similar open-face features to those of the ten-vertex *isonido* compounds described here. As for the *isonido* compound **2**, however, the metal hydride in compound **3** was also not locatable from the X-ray data.[30] However, HYDEX-type[32,33] calculations on this *closo* species give a potential well that is typical for a terminal iridium hydride, confirming the terminal position proposed in ref. 30. A drawing of the structure of the *closo* compound **3** is shown in Fig. 2.

Table 1 Selected interatomic distances (pm) for [7,7,9-$(PPh_3)_3$-*isonido*-7-IrB_9H_{10}] **2** with estimated standard deviations (e.s.d.s) in parentheses

P(1)–Ir(7)	235.5(4)	P(2)–Ir(7)	234.3(4)
B(2)–Ir(7)	235.9(12)	B(3)–Ir(7)	219.3(11)
B(4)–Ir(7)	234.3(12)	B(8)–Ir(7)	232.0(11)
B(10)–Ir(7)	230.4(11)		
C(111)–P(1)	184.6(6)	C(121)–P(1)	184.6(7)
C(131)–P(1)	184.2(7)		
C(211)–P(2)	184.5(7)	C(221)–P(2)	184.7(7)
C(231)–P(2)	185.7(7)		
B(9)–P(3)	189.7(11)	C(311)–P(3)	180.7(7)
C(321)–P(3)	180.4(7)	C(331)–P(3)	181.9(7)
B(2)–B(1)	180.6(16)	B(3)–B(1)	165.8(17)
B(4)–B(1)	182.8(17)	B(5)–B(1)	180.1(17)
B(6)–B(1)	181.4(16)	B(3)–B(2)	179.1(17)
B(6)–B(2)	178.4(16)	B(10)–B(2)	177.5(15)
B(4)–B(3)	177.9(16)	B(5)–B(4)	182.5(16)
B(8)–B(4)	176.6(16)	B(6)–B(5)	183.0(16)
B(8)–B(5)	177.9(15)	B(9)–B(5)	167.8(16)
B(9)–B(6)	170.9(15)	B(10)–B(6)	182.1(14)
B(9)–B(8)	164.6(15)	B(10)–B(9)	168.4(14)

Similar calculations for the new compound **2**, however, did not show any markedly deep potential wells, in particular either (*a*) for a terminal iridium hydride pointing away from the Ir(7)–B(8)–B(10) face in a manner related to that in the *closo* compound **3**, (*b*) for an iridium hydride edge-bridging to the boron atoms in the face, or (*c*) for an edge-bridging hydride associated with the B(8)–B(9)–B(10) face. Additionally, therefore, the possibility cannot be excluded that the hydrogen atoms are in face-capping B(8)–B(9)–B(10) and Ir(7)–B(8)–B(10) positions, rather than edge-bridging positions.

Additional information derives from the bis(phosphine)iridium geometry. In the *closo* compound **3** the P–Ir–P plane is tilted at 48(2)° with respect to the B(2)–B(4)–B(8)–B(10) plane in order to accommodate the terminal hydride (numbering system **VIII** as in compound **2** to facilitate comparison). In the *isonido* compound **2**, by contrast, the angle is 86.6(3)°, thereby suggesting that the hydride is not terminal and is therefore bridging to atoms in the open face. Although a position bridging in the other direction, towards atom B(3), also cannot be completely excluded, it seems to us unlikely.

Table 4 shows a comparison of infrared stretching bands for a range of iridaboranes with bridging and terminal iridium hydrides. The usual range for terminal hydrides is *ca.* 2050–2300 cm^{-1} with absorptions of medium intensity, whereas the *isonido* compound **2** features a broad, weak absorption at 1980 cm^{-1} of intensity comparable to the phenyl ring overtones which also occur in this region. Absorptions arising from bridging Ir–H–B systems are however in our experience not generally observable for most large iridaboranes (see, for example, the compounds listed in Table 4), and the presence of a weak absorption may therefore indicate a bridging hydride with a degree of terminal character. In this context again the *closo* compound **3** seems to be anomalous, with no infrared absorption observed for its reasonably proposed terminal hydride;[30] on this basis some Ir–H–B bridging interaction

Table 2 Selected angles (°) between interatomic vectors for compound **2** with e.s.d.s in parentheses

P(2)–Ir(7)–P(1)	98.0(2)	B(2)–Ir(7)–P(1)	156.0(2)	B(1)–B(4)–Ir(7)	98.2(6)	B(3)–B(4)–Ir(7)	62.5(5)
B(2)–Ir(7)–P(2)	96.1(3)	B(3)–Ir(7)–P(1)	109.9(4)	B(3)–B(4)–B(1)	54.7(7)	B(5)–B(4)–Ir(7)	111.2(7)
B(3)–Ir(7)–P(2)	117.6(4)	B(3)–Ir(7)–B(2)	46.2(4)	B(5)–B(4)–B(1)	59.1(7)	B(5)–B(4)–B(3)	110.5(8)
B(4)–Ir(7)–P(1)	93.8(4)	B(4)–Ir(7)–P(2)	162.9(3)	B(8)–B(4)–Ir(7)	67.1(5)	B(8)–B(4)–B(1)	102.9(8)
B(4)–Ir(7)–B(2)	68.9(4)	B(4)–Ir(7)–B(3)	46.0(4)	B(8)–B(4)–B(3)	118.5(8)	B(8)–B(4)–B(5)	59.4(6)
B(8)–Ir(7)–P(1)	101.2(3)	B(8)–Ir(7)–P(2)	143.0(2)	B(4)–B(5)–B(1)	60.6(7)	B(6)–B(5)–B(1)	59.9(7)
B(8)–Ir(7)–B(2)	78.3(4)	B(8)–Ir(7)–B(3)	84.9(4)	B(6)–B(5)–B(4)	103.7(7)	B(8)–B(5)–B(1)	103.5(7)
B(8)–Ir(7)–B(4)	44.5(3)	B(10)–Ir(7)–P(1)	151.3(2)	B(8)–B(5)–B(4)	58.7(6)	B(8)–B(5)–B(6)	95.4(7)
B(10)–Ir(7)–P(2)	95.3(3)	B(10)–Ir(7)–B(2)	44.7(3)	B(9)–B(5)–B(1)	110.8(8)	B(9)–B(5)–B(4)	108.9(8)
B(10)–Ir(7)–B(3)	85.8(5)	B(10)–Ir(7)–B(4)	79.9(4)	B(9)–B(5)–B(6)	58.1(6)	B(9)–B(5)–B(8)	56.8(6)
B(10)–Ir(7)–B(8)	55.1(4)			B(2)–B(6)–B(1)	60.3(7)	B(5)–B(6)–B(1)	59.2(7)
B(3)–B(1)–B(2)	62.1(7)	B(4)–B(1)–B(2)	94.0(7)	B(5)–B(6)–B(2)	102.8(8)	B(9)–B(6)–B(1)	108.8(8)
B(4)–B(1)–B(3)	61.1(7)	B(5)–B(1)–B(2)	103.1(7)	B(9)–B(6)–B(2)	108.7(7)	B(9)–B(6)–B(5)	56.5(6)
B(5)–B(1)–B(3)	117.7(8)	B(5)–B(1)–B(4)	60.4(7)	B(10)–B(6)–B(1)	103.0(7)	B(10)–B(6)–B(2)	59.0(6)
B(6)–B(1)–B(2)	59.0(7)	B(6)–B(1)–B(3)	117.6(8)	B(10)–B(6)–B(5)	94.4(7)	B(10)–B(6)–B(9)	56.9(6)
B(6)–B(1)–B(4)	104.2(7)	B(6)–B(1)–B(5)	60.8(7)	B(4)–B(8)–Ir(7)	68.4(5)	B(5)–B(8)–Ir(7)	114.1(6)
B(1)–B(2)–Ir(7)	98.2(6)	B(3)–B(2)–Ir(7)	62.0(5)	B(5)–B(8)–B(4)	62.0(6)	B(9)–B(8)–Ir(7)	112.5(6)
B(3)–B(2)–B(1)	54.9(6)	B(6)–B(2)–Ir(7)	112.6(7)	B(9)–B(8)–B(4)	113.4(8)	B(9)–B(8)–B(5)	58.5(6)
B(6)–B(2)–B(1)	60.7(7)	B(6)–B(2)–B(3)	112.4(8)	B(5)–B(9)–P(3)	129.8(7)	B(6)–B(9)–P(3)	127.5(7)
B(10)–B(2)–Ir(7)	66.0(5)	B(10)–B(2)–B(1)	105.2(8)	B(6)–B(9)–B(5)	65.4(7)	B(8)–B(9)–P(3)	126.8(7)
B(10)–B(2)–B(3)	118.4(8)	B(10)–B(2)–B(6)	61.5(6)	B(8)–B(9)–B(5)	64.7(7)	B(8)–B(9)–B(6)	105.5(8)
B(1)–B(3)–Ir(7)	110.0(7)	B(2)–B(3)–Ir(7)	71.8(5)	B(10)–B(9)–P(3)	124.0(7)	B(10)–B(9)–B(5)	105.7(8)
B(2)–B(3)–B(1)	63.0(7)	B(4)–B(3)–Ir(7)	71.4(6)	B(10)–B(9)–B(6)	64.9(6)	B(10)–B(9)–B(8)	79.9(7)
B(4)–B(3)–B(1)	64.2(7)	B(4)–B(3)–B(2)	96.3(8)	B(2)–B(10)–Ir(7)	69.3(5)	B(6)–B(10)–Ir(7)	113.6(6)
				B(6)–B(10)–B(2)	59.5(6)	B(9)–B(10)–Ir(7)	111.7(6)
				B(9)–B(10)–B(2)	110.2(7)	B(9)–B(10)–B(6)	58.2(6)

Table 3 Measured available[a] multielement NMR data for compounds **2**,[b] **5**,[b] **6**,[b] $[(PPh_3)_2IrB_9H_7(OMe)(PPh_3)]$[c] **9** and $[(PPh_3)(Ph_2P\overline{C_6H_4)IrB}_8H_6(OMe)C(OH)]$[d] **8**

Compound **2**			Compound **5**		Compound **6**				Compound **9**		Compound **8**	
$\delta(^{11}B)$	$\delta(^{1}H)$[e]	$\delta(^{1}H)$[f]	$\delta(^{11}B)$	$\delta(^{1}H)$	$\delta(^{11}B)$			$\delta(^{1}H)$	$\delta(^{11}B)$	$\delta(^{1}H)$	$\delta(^{11}B)$	$\delta(^{1}H)$
+25.4	+6.45	+6.48	+59.7	+6.71	*ca.* +30.0			+6.75	+56.2	*i*	+63.9	*i*
−7.0	+2.29[h]	+2.28	+29.0	*i*	*ca.* +10.5			+4.17	+23.2	+4.83	+50.1	*i*
−7.0	+2.29[h]	+2.28	+23.6	*i*	*ca.* −0.5	(4)		+0.02	+23.2	+4.83	+7.9	+3.24
−8.2	+3.48	+3.43	+9.5	+3.01	*ca.* −7.0		*g*	+0.21	−0.8	+2.83	−0.2	+3.24
−11.1[j]	—	—	−5.6[k]	—	*ca.* −13.5(2)			−0.54	−1.8[k]	—	−0.2	+2.62
−30.0	−0.98	−1.02	−8.2	+1.39	*ca.* −24.0(2)			−2.04	−15.8	+0.29	−0.2	+2.78
−30.0	−0.98	−1.02	−16.9	+0.17					−15.8	+0.29	−19.6	−0.8
−32.3	−2.04[l]	−2.13	−19.1	+0.60					−22.9	−1.44	−20.7	−0.49
−32.3	−2.04[l]	−2.13	−26.8	−1.06					−22.9	−1.44	*q*	—
		−4.37						−4.07[m]				
	−6.65[m,n]	−8.70[o]						−8.59[p]				

[a] In some cases (see footnote *g*) not all ^{11}B and ^{1}H data were unequivocally measurable; in all other cases ^{1}H resonances were related to their directly bound ^{11}B atoms by ^{1}H-$\{^{11}B\}$ selective experiments. [b] ^{31}P NMR data for CD_2Cl_2 solutions: compound **2** (−41 °C), $\delta(^{31}P)$ +14.8 (relative intensity 2), and +16 (broad, relative intensity 1); **5** (−40 °C), sharp singlets at $\delta(^{31}P)$ +46.7 and +31.0 and a broad resonance at *ca.* +12; **6** (−40 °C), sharp singlets at $\delta(^{31}P)$ +26.0 and +12.1 with a broad resonance at *ca.* +12. [c] Data from ref. 19. ^{31}P NMR spectrum (CD_2Cl_2 solution at −40 °C): $\delta(^{31}P)$ + 34.4 (relative intensity 2) with a broad resonance at $\delta(^{31}P)$ *ca.* +12 (relative intensity 1). [d] Data from ref. 19. ^{31}P NMR spectrum (CD_2Cl_2 solution at −48 °C): $\delta(^{31}P)$ +26.6 and +26.0, $^{2}J(^{31}P$–$^{31}P)$ 17 Hz. [e] Saturated CD_2Cl_2 solution at +21 °C. [f] Saturated CD_2Cl_2 solution at −84 °C. [g] Boron-11 (measured at 32 MHz) and ^{1}H (measured at 100 Mz) resonances are not related by selective ^{1}H-$\{^{11}B\}$ experiments. It was also not possible to resolve all nine boron resonances and all terminal proton resonances (see text). Relative intensities in parentheses. [h] Doublet structure; splitting 10.8 ± 0.5 Hz. [i] *exo*-Terminal proton resonance absent because of substituents. [j] Doublet $^{2}J(^{31}P$–$^{31}B)$ 185 Hz. [k] Doublet $^{2}J(^{31}P$–$^{11}B)$ 160 Hz. [l] Triplet structure; splitting *ca.* 11 Hz. [m] Shows coupling to boron. [n] $w_{\frac{1}{2}}$ = 46 Hz for ^{1}H spectrum and 37 Hz for ^{1}H-$\{^{31}P\}$ spectrum. [o] Triplet $^{2}J(^{31}P$–$^{1}H)_{cis}$ *ca.* 18 Hz. [p] Two overlapping doublets, $^{2}J(^{31}P$–$^{1}H)_{cis}$ 18 and 25 Hz. [q] Ninth cluster vertex occupied by carbon atom.

Table 4 The M–H and M–H–B proton NMR chemical shifts and infrared stretching bands for compound **2** and other iridaboranes

	$\delta(^{1}H)$		ν_{max}/cm^{-1}	
Compound	M–H	M–H–B	M–H	M–H–B
1	−12.30	−11.08, −6.64	2100m	*b*
a	−14.65	−8.49	2380m	*b*
c	−13.10	−8.89, −6.46	2115m	*b*
d	−15.52	−8.43	2185m	*b*
e	−16.08	*f*	2060m	*f*
2		−8.75		1980w

[a] $[5,7$-$(PPh_3)_2$-5-H-5-$(Ph_2PC_6H_4)$-*nido*-5-$IrB_9H_{10}]$, ref. 8. [b] Not observed. [c] $[6,8$-$(PPh_3)_2$-6-H-6-$(Ph_2PC_6H_4)$-*nido*-$IrB_9H_{10}]$, ref. 8. [d] $[7,7$-$(PMe_3)_2$-9-H-9-(PPh_3)-9-$(Ph_2PC_6H_4)$-*nido*-7,9-$PtIrB_9H_{10}]$, ref. 9. [e] $[4$-(CO)-4-H-4,4-$(PMe_3)_2$-*arachno*-4-$IrB_8H_{12}]$, ref. 29. [f] No M–H–B bridging protons in the compound.

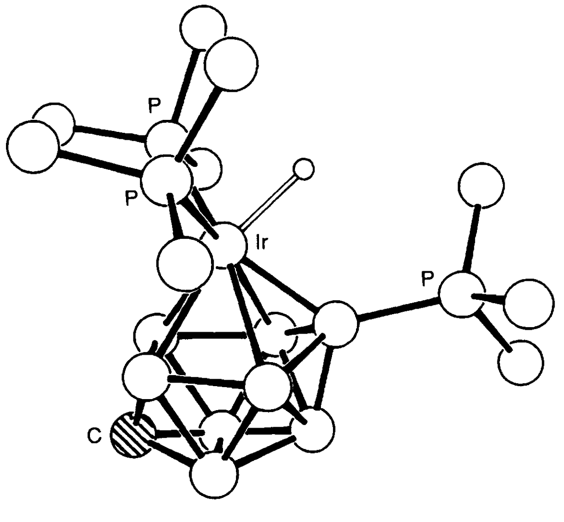

Fig. 2 An ORTEP drawing of $[1,2,2$-$(PPh_3)_3$-2-H-*closo*-2,10-$IrCB_8H_{10}]$ **3**[30] showing the position of the terminal iridium hydride as determined from HYDEX-type potential-well calculations[32,33] using data from ref. 30

cannot be completely ruled out for this conventional ten-vertex *closo* compound also.

On balance we would suggest that the hydrogen atoms in the new *isonido* compound **2** are bridging on the open face as illustrated in Fig. 1 (although a face-capping configuration is probably energetically very similar). There is probably also low-temperature exchange of the Ir–H–B hydrogen atom between the two open-face Ir(7)–B(8) and Ir(7)–B(10) sites, and concomitantly of the B–H–B hydrogen atom between the B(8)–B(9) and B(9)–B(10) sites. This is suggested by the apparent retention in the NMR spectra of time-averaged mirror-plane symmetry at temperatures below which exchange between the IrHB and BHB types of position is frozen. Related multistage hydride fluxionalities are known in other metallaborane systems, for example in some rhena- and tungsta-boranes.[34–36]

In any event, the *isonido* compound **2** poses interesting structural questions, and we thought further examples of this structural type would be of interest. Our attempts to produce further *isonido*-iridadecaboranes have so far derived from the hypothesis that the formation of *isocloso*-iridadecaboranes such as $[(PPh_3)(Ph_2P\overline{C_6H_4)HIrB}_9H_8]$ from *nido*-iridadecaboranes such as $[6$-(PPh_3)-6-$(Ph_2P\overline{C_6H_4)}$-6-H-*nido*-6-$\overline{Ir}B_9H_{12}]$ would proceed through an *isonido*-type intermediate [equations (1) and (2); see also structures **I**, **V** and **IV** in Scheme 1].[4]

$$[(PPh_3)(Ph_2P\overline{C_6H_4)_2HIrB}_9H_{12}] \longrightarrow \underset{isonido}{\{(PPh_3)(Ph_2P\overline{C_6H_4)HIrB}_9H_{10}\}} + H_2 \quad (1)$$

$$\{(PPh_3)(Ph_2P\overline{C_6H_4)HIrB}_9H_{10}\} \longrightarrow \underset{isocloso}{[(PPh_3)(Ph_2P\overline{C_6H_4)HIrB}_9H_8]} + H_2 \quad (2)$$

This reaction may be regarded formally as the loss of the four bridging hydrogen atoms, and it is supposed that one molecule of dihydrogen would be lost to give an *isonido* intermediate followed followed by loss of a second molecule of dihydrogen to give the *isocloso* species.[4] If this was so it would follow that a phosphine-substituted *nido*-iridadecaborane cluster compound, with a B-phosphine ligand instead of B–H(*exo*) plus one

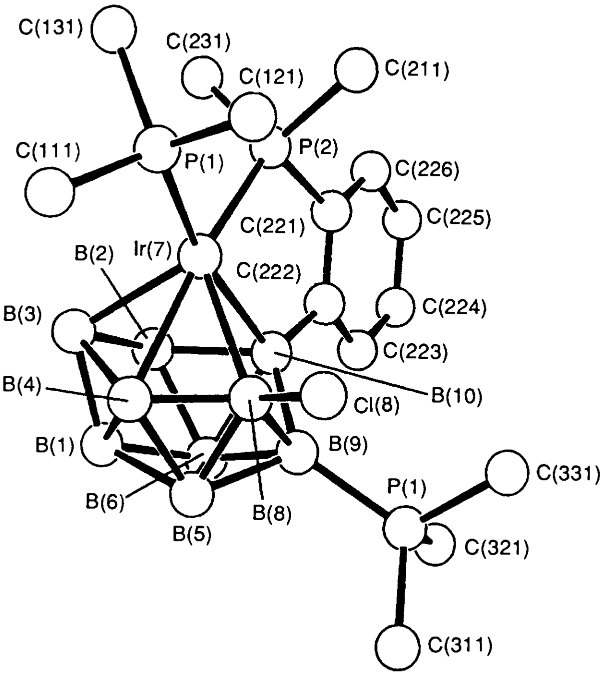

Fig. 3 An ORTEP diagram of [8-Cl-7,9-$(PPh_3)_2$-7-(*o*-Ph_2P-C_6H_4)-*isonido*-7-IrB_9H_6-10] **5** with P-phenyl group atoms (except for the *ipso* carbon ones) omitted for clarity. All heavy atoms were located and ^1H-{^{11}B} NMR spectroscopy reveals the presence of terminal hydrogen atoms on six of the boron atoms. The open face of the cluster, in contrast to compounds **2** (Fig. 1) and **6** (Fig. 4), does not have bridging hydrogen atoms

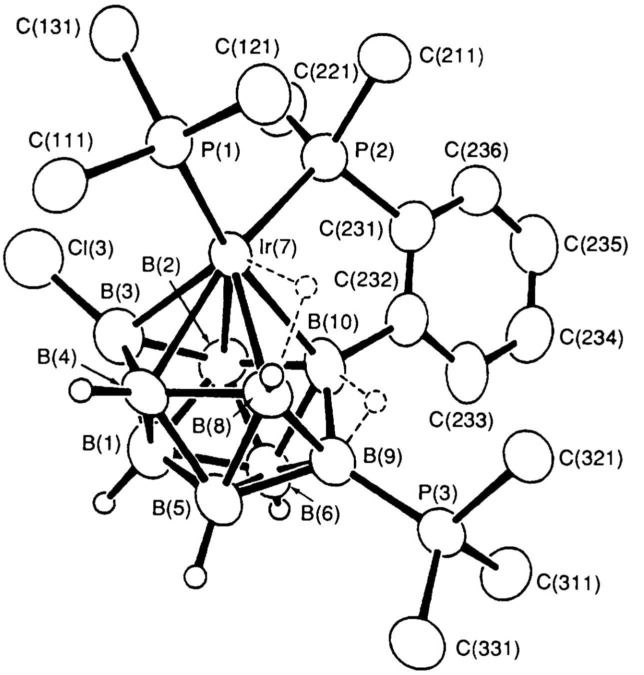

Fig. 4 An ORTEP drawing of the molecular structure of [3-Cl-7,9-$(PPh_3)_2$-7-(*o*-$Ph_2PC_6H_4$)-*isonido*-7-IrB_9H_8-10] **6a** with P-phenyl group atoms (except for the *ipso* carbon ones) omitted for clarity. In the crystal selected the B(3) vertex was bound to a hydrogen atom (compound **6** proper) or a chlorine atom (compound **6a**) with an occupancy ratio of 25:75. All atoms were located with the exception of the two hydrogen atoms associated with the open face. Their positions (hatched lines) are suggested from ^1H NMR data and by a comparison with compound **2** (see text)

Table 5 Selected interatomic distances (pm) for [8-Cl-7,9-$(PPh_3)_2$-7-(*o*-$Ph_2PC_6H_4$)-*isonido*-7-IrB_9H_6-10] **5** with e.s.d.s in parentheses

P(1)–Ir(7)	237.9(7)	P(2)–Ir(7)	234.0(7)
B(2)–Ir(7)	241.1(21)	B(3)–Ir(7)	215.3(23)
B(4)–Ir(7)	236.5(25)	B(8)–Ir(7)	220.0(22)
B(10)–Ir(7)	231.6(24)		
C(111)–P(1)	181.9(14)	C(121)–P(1)	182.6(11)
C(131)–P(1)	181.4(14)		
C(211)–P(2)	183.5(13)	C(221)–P(2)	181.8(12)
C(231)–P(2)	181.7(15)		
B(9)–P(3)	191.7(22)	C(311)–P(3)	180.4(14)
C(321)–P(3)	181.2(13)	C(331)–P(3)	182.6(13)
B(8)–Cl(8)	191.6(26)	B(2)–B(1)	186.4(33)
B(3)–B(1)	172.8(32)	B(4)–B(1)	193.0(33)
B(5)–B(1)	176.8(31)	B(6)–B(1)	176.7(34)
B(3)–B(2)	186.4(32)	B(6)–B(2)	182.1(34)
B(10)–B(2)	183.3(34)	B(4)–B(3)	183.0(32)
B(5)–B(4)	177.7(33)	B(8)–B(4)	170.2(35)
B(6)–B(5)	183.8(32)	B(8)–B(5)	168.9(30)
B(9)–B(5)	177.8(31)	B(9)–B(6)	173.5(30)
B(10)–B(6)	185.2(36)	B(9)–B(8)	167.2(33)
B(10)–B(9)	173.3(35)	C(222)–B(10)	154.7(29)

bridging hydrogen atom, should therefore eliminate dihydrogen according to equation (3) to result in a more stable *isonido*

$$[H(PPh_3)_2IrB_9H_{11}(PPh_3)] \longrightarrow [(PPh_3)_2IrB_9H_{10}(PPh_3)] + H_2 \quad (3)$$

species. This would in principle have an equivalent formulation to compound **2**, and therefore be possibly isostructural with it.

A compound of the precise $[H(PPh_3)_2IrB_9H_{11}(PPh_3)]$ formulation is not available, but we were able to test the hypothesis using the closely related B-*ortho*-cyclophenylated derivative [5,7-$(PPh_3)_2$-5-H-5-(*o*-$Ph_2PC_6H_4$)-*nido*-5-IrB_9H_{10}-2] **4**. When heated at *ca.* 343 K in 1,1,2,2-tetrachloroethane solution for 1 h compound **4** gave several highly coloured (yellow, red, purple, blue) reasonably air-stable products in variable and very small yield. These have proved to be very difficult to separate reliably in pure form, but we have been able to isolate and reasonably characterise two of them (compounds **5** and **6**) as *isonido*-type species by single-crystal X-ray diffraction analyses and NMR spectroscopy.

Fig. 3 shows an ORTEP diagram obtained for the deep purple compound [8-Cl-7,9-$(PPh_3)_2$-7-(*o*-Ph_2-PC_6H_4)-*isonido*-7-IrB_9H_6-10] **5**, and Tables 5 and 6 show listings of interatomic distances and angles. The diffraction analysis on compound **6** showed that the royal blue crystal of [7,9-$(PPh_3)_2$-7-(*o*-$Ph_2PC_6H_4$)-*isonido*-7-IrB_9H_9-10] used contained *ca.* 25 mole % of its 3-chlorinated derivative [3-Cl-7,9-$(PPh_3)_2$-7-(*o*-$Ph_2PC_6H_4$)-*isonido*-7-IrB_9H_8-10] **6a**. In view of the small samples available, it is not certain whether this may have arisen from cocrystallisation of an initial reaction product, or from reaction with the $CHCl_3$ solvent used in the crystallisation. In this context, we note that both compounds **2** and **6** showed signs of slow reaction with $CHCl_3$ (compare rhena- and cobalta-boranes in refs. 35 and 37), whereas **5** was crystallised from CH_2Cl_2 with which no reaction was apparent and **2** was found similarly to be unreactive with CH_2Cl_2. An ORTEP diagram of **6a** is shown in Fig. 4 and interatomic separations and angles are listed in Tables 7 and 8.

In view of the uncertainty about the interesting nature and the precise positions of the bridging hydrogen atoms in compound **2**, it was important to investigate compounds **5** and **6** for this type of feature. Our investigation was however hindered by the low yields of these two species (*ca.* 5%) and the presence of other low-yield products with closely related properties, all generated from a material (compound **4**) itself obtainable only

Table 6 Selected angles (°) for compound **5** with e.s.d.s in parentheses

P(2)–Ir(7)–P(1)	98.4(3)	B(2)–Ir(7)–P(1)	148.9(5)	B(4)–B(5)–B(1)	65.9(13)	B(6)–B(5)–B(1)	58.6(13)
B(2)–Ir(7)–P(2)	94.5(7)	B(3)–Ir(7)–P(1)	103.2(6)	B(6)–B(5)–B(4)	108.4(15)	B(8)–B(5)–B(1)	105.3(15)
B(3)–Ir(7)–P(2)	127.6(7)	B(3)–Ir(7)–B(2)	47.8(7)	B(8)–B(5)–B(4)	58.7(14)	B(8)–B(5)–B(6)	96.3(15)
B(4)–Ir(7)–P(1)	94.6(6)	B(4)–Ir(7)–P(2)	167.0(5)	B(9)–B(5)–B(1)	109.5(15)	B(9)–B(5)–B(4)	111.2(15)
B(4)–Ir(7)–B(2)	73.8(8)	B(4)–Ir(7)–B(3)	47.5(7)	B(9)–B(5)–B(6)	57.3(12)	B(9)–B(5)–B(8)	57.6(13)
B(8)–Ir(7)–P(1)	109.8(7)	B(8)–Ir(7)–P(2)	130.5(6)	B(2)–B(6)–B(1)	62.6(13)	B(5)–B(6)–B(1)	58.7(13)
B(8)–Ir(7)–B(2)	82.0(9)	B(8)–Ir(7)–B(3)	85.0(9)	B(5)–B(6)–B(2)	104.9(15)	B(9)–B(6)–B(1)	111.6(16)
B(8)–Ir(7)–B(4)	43.6(8)	B(10)–Ir(7)–P(1)	165.0(6)	B(9)–B(6)–B(2)	110.1(16)	B(9)–B(6)–B(5)	59.6(12)
B(10)–Ir(7)–P(2)	80.5(7)	B(10)–Ir(7)–B(2)	45.6(8)	B(10)–B(6)–B(1)	107.8(16)	B(10)–B(6)–B(2)	59.9(13)
B(10)–Ir(7)–B(3)	89.0(9)	B(10)–Ir(7)–B(4)	87.1(9)	B(10)–B(6)–B(5)	99.4(15)	B(10)–B(6)–B(9)	57.8(13)
B(10)–Ir(7)–B(8)	62.0(10)			Cl(8)–B(8)–Ir(7)	113.2(11)	B(4)–B(8)–Ir(7)	73.4(13)
B(3)–B(1)–B(2)	62.4(13)	B(4)–B(1)–B(2)	98.2(13)	B(4)–B(8)–Cl(8)	113.2(15)	B(5)–B(8)–Ir(7)	116.4(15)
B(4)–B(1)–B(3)	59.7(12)	B(5)–B(1)–B(2)	105.9(15)	B(5)–B(8)–Cl(8)	125.3(14)	B(5)–B(8)–B(4)	63.2(14)
B(5)–B(1)–B(3)	112.7(16)	B(6)–B(1)–B(2)	60.1(13)	B(9)–B(8)–Ir(7)	109.5(14)	B(9)–B(8)–Cl(8)	118.0(16)
B(6)–B(1)–B(3)	116.6(16)	B(6)–B(1)–B(4)	104.9(14)	B(9)–B(8)–B(4)	120.8(18)	B(9)–B(8)–B(5)	63.9(14)
B(6)–B(1)–B(5)	62.7(14)			B(5)–B(9)–P(3)	123.4(14)	B(6)–B(9)–P(3)	126.2(14)
B(1)–B(2)–Ir(7)	94.1(11)	B(3)–B(2)–Ir(7)	58.8(9)	B(6)–B(9)–B(5)	63.1(13)	B(8)–B(9)–P(3)	129.0(14)
B(3)–B(2)–B(1)	55.2(13)	B(6)–B(2)–Ir(7)	104.7(12)	B(8)–B(9)–B(5)	58.5(13)	B(8)–B(9)–B(6)	101.0(16)
B(6)–B(2)–B(1)	57.3(13)	B(6)–B(2)–B(3)	107.6(16)	B(10)–B(9)–P(3)	128.6(15)	B(10)–B(9)–B(5)	106.4(15)
B(10)–B(2)–Ir(7)	64.5(10)	B(10)–B(2)–B(1)	104.5(16)	B(10)–B(9)–B(6)	64.5(14)	B(10)–B(9)–B(8)	86.2(14)
B(10)–B(2)–B(3)	116.0(14)	B(10)–B(2)–B(6)	60.9(14)	B(2)–B(10)–Ir(7)	70.0(11)	B(6)–B(10)–Ir(7)	107.4(14)
B(1)–B(3)–Ir(7)	108.0(13)	B(2)–B(3)–Ir(7)	73.4(10)	B(6)–B(10)–B(2)	59.2(14)	B(9)–B(10)–Ir(7)	102.3(13)
B(2)–B(3)–B(1)	62.4(13)	B(4)–B(3)–Ir(7)	72.3(11)	B(9)–B(10)–B(2)	109.4(18)	B(9)–B(10)–B(6)	57.7(13)
B(4)–B(3)–B(1)	65.6(13)	B(4)–B(3)–B(2)	101.9(15)	C(222)–B(10)–Ir(7)	115.6(15)	C(222)–B(10)–B(2)	113.5(18)
B(3)–B(4)–Ir(7)	60.2(11)	B(5)–B(4)–Ir(7)	105.5(13)	C(222)–B(10)–B(6)	130.1(16)	C(222)–B(10)–B(9)	129.9(18)
B(5)–B(4)–B(3)	107.5(14)	B(8)–B(4)–Ir(7)	63.1(11)				
B(8)–B(4)–B(3)	112.7(17)	B(8)–B(4)–B(5)	58.0(13)				

Table 7 Selected interatomic distances for $[3\text{-}Cl_{0.25}\text{-}7,9\text{-}(PPh_3)_2\text{-}7\text{-}(o\text{-}Ph_2PC_6H_4)$-*isonido*-$7\text{-}IrB_9H_{8.75}\text{-}10]$ **6** with e.s.d.s in parentheses

P(1)–Ir(7)	234.8(4)	P(2)–Ir(7)	230.8(4)
B(2)–Ir(7)	234.5(11)	B(3)–Ir(7)	217.3(13)
B(4)–Ir(7)	235.5(12)	B(8)–Ir(7)	231.7(10)
B(10)–Ir(7)	228.9(11)		
C(111)–P(1)	183.3(7)	C(121)–P(1)	184.7(6)
C(131)–P(1)	181.2(7)		
C(211)–P(2)	184.0(7)	C(221)–P(2)	184.2(6)
C(231)–P(2)	180.7(6)		
B(9)–P(3)	189.7(10)	C(311)–P(3)	180.1(7)
C(321)–P(3)	182.5(7)	C(331)–P(3)	180.9(7)
B(2)–B(1)	184.3(17)	B(3)–B(1)	171.3(17)
B(4)–B(1)	186.4(15)	B(5)–B(1)	181.2(13)
B(6)–B(1)	181.0(15)	B(3)–B(2)	180.9(16)
B(6)–B(2)	182.4(15)	B(10)–B(2)	178.2(13)
B(4)–B(3)	178.5(13)	Cl(3)–B(3)	179.0(16)
B(5)–B(4)	185.0(15)	B(8)–B(4)	179.4(14)
B(6)–B(5)	181.9(14)	B(8)–B(5)	182.8(16)
B(9)–B(5)	173.2(15)	B(9)–B(6)	171.5(13)
B(10)–B(6)	181.9(16)	B(9)–B(8)	167.7(14)
B(10)–B(9)	170.9(14)	C(232)–B(10)	159.4(12)

in very low yield.[4] The problem was compounded somewhat by the susceptibility to chlorination in the solvent systems used. There have been particular difficulties in matching the particular single crystals selected for X-ray diffraction analysis with the ^1H, ^{11}B and ^{31}P NMR properties of larger samples that were generally obtained as mixtures difficult to separate completely. The NMR problems are compounded further by the broad ^{11}B linewidths of these relatively bulky molecules.

The measured ^{11}B and $^1H\text{-}\{^{11}B\}$ NMR spectra of samples of the blue compound **6** (data summarised in Table 3) did not completely resolve all the individual boron and terminal hydrogen atom resonances. The data obtained are, however, not inconsistent with the solid-state X-ray structure, and unequivocally show two proton resonances with chemical shifts very similar to those observed at low temperature for the bridging positions in compound **2** [*viz.* at $\delta(^1H)$ −4.07 and −8.59 for **6**, *versus* −4.37 and −8.70 for **2**]. The resonance at δ −8.59 for compound **6** is coupled to two (inequivalent) phosphorus atoms and shows no coupling to boron. The two proton resonances did not show any evidence for fluxionality; presumably this would be restricted by the *ortho*-cycloboronated phenylene ring in this particular cluster. As with compound **2**, XHYDEX potential-well calculations on the molecule were inconclusive.

The NMR properties of compound **5** were somewhat better defined, with all boron and terminal hydrogen atom resonances related by selective $^1H\text{-}\{^{11}B\}$ spectroscopy. In contrast to **2** and **6**, the compound appeared not to show any bridging hydrogen or terminal-type iridium hydride resonances. However, the absence of bridging hydrogen atoms in the ten-vertex *isonido* system has precedent in the red iridaborane $[3\text{-}(OEt)\text{-}4,9\text{-}(PPh_3)_2\text{-}7\text{-}Cl\text{-}7\text{-}(o\text{-}Ph_2PC_6H_4)$-*isonido*-$7\text{-}IrB_9H_5\text{-}8]$[7] **7** and in the purple iridacarbaborane $[(PPh_3)(Ph_2PC_6H_4)IrB_8H_6(OMe)C(OH)]$[6] **8** and some of its congeners[19] such as $[(PPh_3)_2IrB_9H_7(OMe)(PPh_3)]$ **9**.

These two different ten-vertex *isonido* types, with two bridging-type hydrogen atoms (compounds **2** and **6**), or without these two extra hydrogen atoms (compounds **5**, **8** and **10**), appear to have characteristically different ^{11}B NMR shielding patterns (Table 3). Although most of the individual resonances are unassigned to particular cluster sites in all the compounds examined, and the data in the intermediate ^{11}B shielding range for compound **6** are not completely certain, it nevertheless appears that the unbridged compounds **5**, **8** and **9** are characterised by a low-field ^{11}B NMR resonance at $\delta(^{11}B)$ *ca.* +60, and that this is absent for the bridged species **2** and **6**. This low-field resonance is readily assigned to the low-connectivity B(3) position adjacent to the metal atom (structure **X**) because this is the substituted one in compounds **8** and **9**.

It is of interest in this context that the 2,3,4 positions in *isocloso* ten-vertex species such as $[(PPh_3)(Ph_2PC_6H_4)HIrB_9H_8]$,[4] $[(C_4H_4)(Ph_2PC_6H_4)IrB_9H_7(PPh_3)]$[38] and $[Cl(H)(PPh_3)RuB_9H_7(PPh_3)_2]$[39] (structure **XI**), the 2,3-positions in *isocloso* eleven-vertex clusters such as $[(C_5Me_5)IrB_{10}H_{10}]$[40] (structure **XII**), and the 2,4,5,7 positions of the *isocloso* nine-vertex cluster $[Cl(H)(PMe_3)_2IrB_8H_7]$[15] (structure **XIII**) also exhibit characteristic low-field resonances. These positions all also have the the low cluster connectivity of four, and also all are

Table 8 Selected angles (°) between interatomic vectors for compound **6** with e.s.d.s in parentheses

P(2)–Ir(7)–P(1)	99.7(2)	B(2)–Ir(7)–P(1)	156.5(2)	B(1)–B(4)–Ir(7)	97.2(6)	B(3)–B(4)–Ir(7)	61.5(6)
B(2)–Ir(7)–P(2)	93.5(3)	B(3)–Ir(7)–P(1)	109.9(4)	B(3)–B(4)–B(1)	55.9(6)	B(5)–B(4)–Ir(7)	109.7(6)
B(3)–Ir(7)–P(2)	125.3(3)	B(3)–Ir(7)–B(2)	47.0(4)	B(5)–B(4)–B(1)	58.4(6)	B(5)–B(4)–B(3)	110.8(7)
B(4)–Ir(7)–P(1)	97.2(3)	B(4)–Ir(7)–P(2)	163.1(2)	B(8)–B(4)–Ir(7)	66.3(5)	B(8)–B(4)–B(1)	103.6(7)
B(4)–Ir(7)–B(2)	70.4(4)	B(4)–Ir(7)–B(3)	46.2(3)	B(8)–B(4)–B(3)	118.6(8)	B(8)–B(4)–B(5)	60.2(6)
B(8)–Ir(7)–P(1)	104.1(3)	B(8)–Ir(7)–P(2)	129.7(3)	B(4)–B(5)–B(1)	61.2(6)	B(6)–B(5)–B(1)	59.8(6)
B(8)–Ir(7)–B(2)	81.6(4)	B(8)–Ir(7)–B(3)	86.5(4)	B(6)–B(5)–B(4)	103.5(7)	B(8)–B(5)–B(1)	104.4(7)
B(8)–Ir(7)–B(4)	45.1(3)	B(10)–Ir(7)–P(1)	155.8(2)	B(8)–B(5)–B(4)	58.4(6)	B(8)–B(5)–B(6)	95.8(7)
B(10)–Ir(7)–P(2)	82.5(3)	B(10)–Ir(7)–B(2)	45.2(3)	B(9)–B(5)–B(1)	109.9(7)	B(9)–B(5)–B(4)	107.4(8)
B(10)–Ir(7)–B(3)	87.4(5)	B(10)–Ir(7)–B(4)	82.4(4)	B(9)–B(5)–B(6)	57.7(6)	B(9)–B(5)–B(8)	56.1(6)
B(10)–Ir(7)–B(8)	58.8(4)			B(2)–B(6)–B(1)	60.9(6)	B(5)–B(6)–B(1)	59.9(6)
B(3)–B(1)–B(2)	61.1(7)	B(4)–B(1)–B(2)	93.9(7)	B(5)–B(6)–B(2)	104.5(7)	B(9)–B(6)–B(1)	110.8(7)
B(4)–B(1)–B(3)	59.7(6)	B(5)–B(1)–B(2)	104.1(7)	B(9)–B(6)–B(2)	108.9(8)	B(9)–B(6)–B(5)	58.6(6)
B(5)–B(1)–B(3)	116.2(8)	B(5)–B(1)–B(4)	60.4(6)	B(10)–B(6)–B(1)	105.0(8)	B(10)–B(6)–B(2)	58.6(6)
B(6)–B(1)–B(2)	59.9(6)	B(6)–B(1)–B(3)	116.4(9)	B(10)–B(6)–B(5)	98.2(7)	B(10)–B(6)–B(9)	57.8(6)
B(6)–B(1)–B(4)	103.3(7)	B(6)–B(1)–B(5)	60.3(6)	B(4)–B(8)–Ir(7)	68.6(5)	B(5)–B(8)–Ir(7)	112.1(5)
B(1)–B(2)–Ir(7)	98.2(6)	B(3)–B(2)–Ir(7)	61.5(5)	B(5)–B(8)–B(4)	61.4(6)	B(9)–B(8)–Ir(7)	108.4(5)
B(3)–B(2)–B(1)	55.9(6)	B(6)–B(2)–Ir(7)	109.6(5)	B(9)–B(8)–B(4)	112.5(7)	B(9)–B(8)–B(5)	59.0(6)
B(6)–B(2)–B(1)	59.1(6)	B(6)–B(2)–B(3)	111.0(7)	B(5)–B(9)–P(3)	123.6(7)	B(6)–B(9)–P(3)	129.9(7)
B(10)–B(2)–Ir(7)	65.7(5)	B(10)–B(2)–B(1)	105.2(6)	B(6)–B(9)–B(5)	63.7(6)	B(8)–B(9)–P(3)	122.3(6)
B(10)–B(2)–B(3)	118.3(7)	B(10)–B(2)–B(6)	60.6(6)	B(8)–B(9)–B(5)	64.8(7)	B(8)–B(9)–B(6)	105.8(7)
B(1)–B(3)–Ir(7)	109.3(7)	B(2)–B(3)–Ir(7)	71.5(6)	B(10)–B(9)–P(3)	129.6(7)	B(10)–B(9)–B(5)	106.1(7)
B(2)–B(3)–B(1)	63.0(7)	B(4)–B(3)–Ir(7)	72.3(5)	B(10)–B(9)–B(6)	64.2(6)	B(10)–B(9)–B(8)	83.8(7)
B(4)–B(3)–B(1)	64.4(6)	B(4)–B(3)–B(2)	97.8(7)	B(2)–B(10)–Ir(7)	69.0(5)	B(6)–B(10)–Ir(7)	112.2(6)
Cl(3)–B(3)–Ir(7)	107.8(8)	Cl(3)–B(3)–B(1)	142.6(8)	B(6)–B(10)–B(2)	60.9(6)	B(9)–B(10)–Ir(7)	108.4(6)
Cl(3)–B(3)–B(2)	127.0(8)	Cl(3)–B(3)–B(4)	133.6(7)	B(9)–B(10)–B(2)	111.2(8)	B(9)–B(10)–B(6)	58.1(6)
				C(232)–B(10)–Ir(7)	113.4(6)	C(232)–B(10)–B(2)	114.4(6)
				C(232)–B(10)–B(6)	127.1(7)	C(232)–B(10)–B(9)	126.2(7)
				C(231)–C(232)–B(10)	119.1(5)	C(233)–C(232)–B(10)	120.9(6)

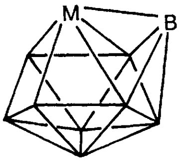

X

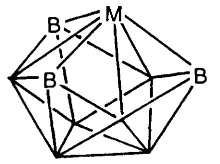

XI

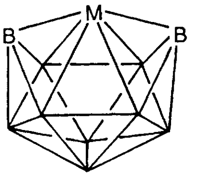

XII

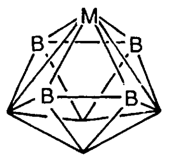

XIII

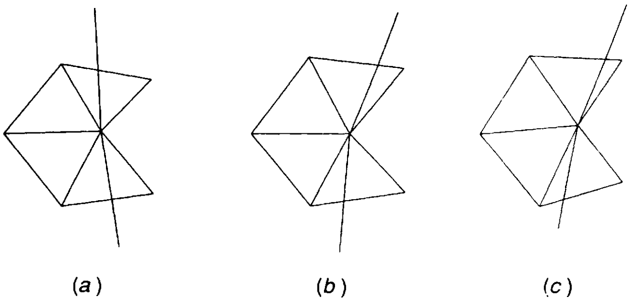
(*a*) (*b*) (*c*)

Fig. 5 ORTEP plots of compounds **2**(*a*), **5**(*b*) and **6**(*c*) viewed perpendicular to the B(2)–B(4)–B(8)–B(10) plane and illustrating the twist of the P(1)–Ir(7)–P(2) plane produced by the presence of an *o*-cycloboronated phosphine group

adjacent to a metal atom in the *isocloso* nine-, ten-, and eleven-vertex cluster shapes that were not recognised in the original Williams–Wade systematic categorisations[1,2] of borane structural patterns mentioned in the Introduction. As also discussed in the Introduction, the *isonido* structures described here also do not fit in with these original structural patterns, and the low ^{11}B shielding may thereby reflect related metal–borane bonding with features common to all four of these '*iso*' structural types (see electron-counting section below). One possibility that we considered was that there might be some relationship between the low ^{11}B shieldings and the shortness of the Ir–B(3) linkage, but in fact there seems to be no significant correlation here.

Comparative NMR spectroscopy on these and the various other highly coloured low-yield reaction products, generally obtained as mixtures, suggests that the other products include several other closely related ten-vertex *isonido*-iridadecaboranes. Some may reversibly isomerise on dissolution (although we believe that this is not the case for the compounds **2**, **5** and **6** reported here). In our hands yields have been variable, all compounds have similar chromatographic properties, and reproduction has been difficult. The compounds appear to vary in the number of iridium bridging or terminal hydrogen atoms (from zero to two), in the incidence of both one- and two-electron *exo* substituents on boron, and in the substituents on the iridium atom. Therefore, although this *isonido* type of cluster is readily formed in the preparative experiments described, the *isonido* reaction products have so far consisted of mixtures of several compounds that are difficult to separate. The problem of separation and characterisation is often exacerbated by the relative abilities of the individual compounds readily to crystallise, and by sensitivities to the chlorinated solvents that are often necessary to effect the separations.

Structural Intercomparisons and the closo $\longrightarrow$ isonido $\longrightarrow$ isocloso *Continuum*.—Apart from the presence of 25% of the 3-chloro derivative in the crystal of compound **6** that was used for the solid-state structure determination, the two hydrogen-bridged compounds **6** and **2** differ only in the incidence of the *o*-phenylene ring (in **6**). Between these two structures the only significant differences in cluster interatomic distances and angles are quite minor ones associated with the effects of the

Table 9 Values of the fold angle (α) between planes Ir(7)–B(8)–B(9) and B(8)–B(9)–B(10) for various clusters *versus* the interatomic distance (*d*) B(8) • • • B(10) (see Fig. 6)

Cluster type		Compound	α/°	*d*/pm	Ref.
closo	a	$[(PPh_3)HIrCB_8H_7(OCOMe)(PPh_3)]$	+18.6(11)	188.9(32)	6
	b	$[H(PPh_3)_2IrCB_8H_{10}(PPh_3)]$ **3**	+9.0(7)	198.6(23)	30
	c	$[(\eta^5\text{-}C_5Me_5)RhB_9H_7(PMe_2Ph)_2]$	+13.5(4)	199.8(8)	41
	d	$[(\eta^5\text{-}C_5Me_5)RhB_9(SMe_2)H_{10}RhB_9H_7(SMe_2)_2]$	+10.5(5)	202.8(12)	42
	e	$[(PH_3)_2(Ph_2PC_6H_4)IrB_9H_7(PPh_3)]$	+13.8(5)	204.9(11)	38
isonido	f	**2**	+8.4(5)	215.8(13)	*
	g	**6**	+6.3(5)	226.2(11)	*
	h	$[Cl(Ph_2PC_6H_4)IrB_9H_5(OEt)(PPh_3)_2]$ **7**	+5.3(4)	229.6(10)	7
	i	**5**	+1.3(11)	232.9(33)	*
isocloso	j	$[(PPh_3)(Ph_2PC_6H_4)IrB_8H_6(OMe)C(OH)]$ **8**	−22.1	269	6
	k	$[H(PPh_3)(Ph_2PC_6H_4)IrB_9H_8]$	−25.1(6)	300.5(14)	4
			−22.2(6)	300.0(13)	
			−23.1(6)	294.7(15)	
	l	$[(C_4H_4)(Ph_2PC_6H_4)IrB_9H_7(PPh_3)]$	−24.9(6)	299.1(13)	38
	m	$[Cl(H)(PPh_3)RuB_9H_7(PPh_3)_2]$	−18.0(4)	287.6(11)	39
			−21.8(4)	297.5(11)	
			−23.4(4)	295.0(12)	

* This work.

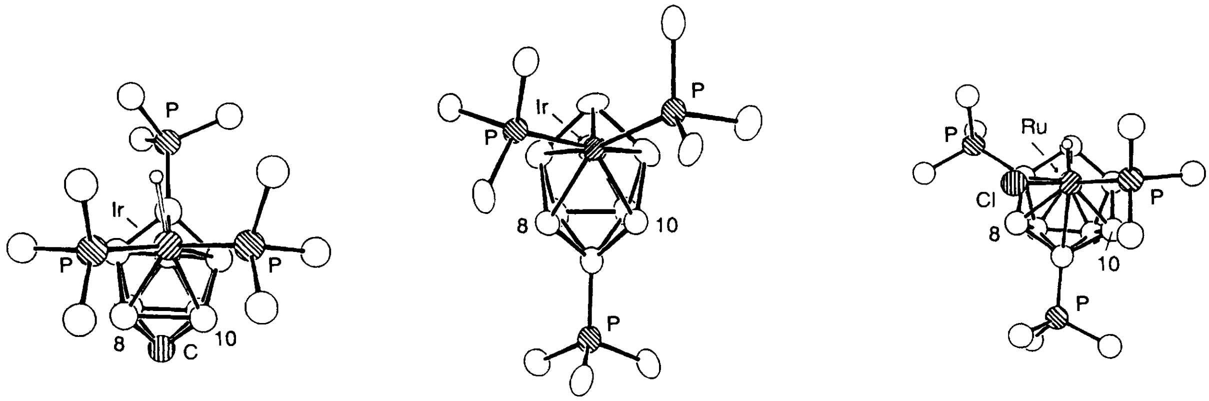

(*a*) (*b*) (*c*)

Fig. 6 The *closo* ⟶ *isonido* ⟶ *isocloso* structural continuum illustrated by ORTEP plots of (*a*) $[H(PPh_3)_3\text{-}\mathit{closo}\text{-}IrCB_8H_{10}]$ **3**, (*b*) $[(PPh_3)_3\text{-}\mathit{isonido}\text{-}IrB_9H_{10}]$ **2** and (*c*) $[Cl(H)(PPh_3)\text{-}\mathit{isocloso}\text{-}RuB_9H_7(PPh_3)_2]$

cyclisation. Thus, although all the Ir–B distances in compound **6** are within 2 pm of those in **2**, there is a twist of the P(1)–Ir(7)–P(2) plane from a position that approximately bisects the B(2)–B(10) and B(4)–B(8) vectors in **2** to a position in which the phosphorus atoms are almost eclipsing the B(2) and B(10) atoms in **6** (Fig. 5). Another difference associated with the cyclisation is that the distance from the iridium to the phosphorus atom P(2) in the orthocycloboronated ring in compound **6** is *ca.* 3.5(4) pm shorter than the Ir–P distances in **2**.

Remarkably, compound **5**, which in contrast to **2** and **6** appears to have no bridging hydrogen atoms, is still geometrically very similar to **2** and **6**. The principle exception to this generalisation is the Ir–B(8) distance which is significantly shorter than in **6** [220.0(22) *versus* 231.7(10) pm]. This could be a consequence of the lack of the bridging hydrogen atom, although the effect of the electronegative chloro-substituent on B(8) in compound **5** may also have a role. Each of the three compounds features five Ir–B interatomic separations within the usual range for iridaborane clusters.[5] Of these separations, four, from Ir(7) to B(2), B(4), B(8) and B(10), are essentially identical, all being within the range of *ca.* 228–236 pm. The fifth, from Ir(7) to the low-connectivity B(3) atom, at *ca.* 217 pm, is however significantly shorter than the others (by *ca.* 15 pm). This difference is also a feature of the two other reported compounds of this *isonido* ten-vertex structural type, the iridacarbaborane **8** and the iridaborane **7**, of which both are in the non-hydrogen-bridged sub-category. In these last two cases the difference is somewhat more extreme (up to *ca.* 24 pm). It is of interest that this shortening also occurs for the equivalent M–B(2) and –B(3) distances in the *closo* 11-vertex geometry from which the *isonido* is formally derived (structure **VI**; see also discussion near structures **X**–**XIII**). Other intracluster distances and angles are within the usual ranges, with the exception of the B(8) • • • B(10) distances which range from *ca.* 216 to 233 pm among these compounds and are taken to be non-bonding, thereby generating the open Ir(7)–B(8)–B(9)–B(10) face and the *isonido* descriptor.

This open face typifies the ten-vertex *isonido* structural type **V** and its dimensions merit comparison (Table 9) with those in its *closo* and *isocloso* congeners **I** and **IV** (Scheme 1). The ORTEP and ORTEP-type diagrams of the clusters are shown in Fig. 6. It can be seen that these can be ordered into a fascinating and gradual progression from a fully closed conventional *closo* bicapped Archimedean-antiprismatic structure through an open square-faced *isonido*-type structure to a fully closed *isocloso* cluster (structures **I** ⟶ **V** ⟶ **IV** Scheme 1). This change is characterised by a diamond–square–diamond[10] flexing of the Ir(7)B(8)B(9)B(10) unit which constitutes the open face in the *isonido* species.

Fig. 7 is a plot of the value of the B(8) • • • B(10) separation in

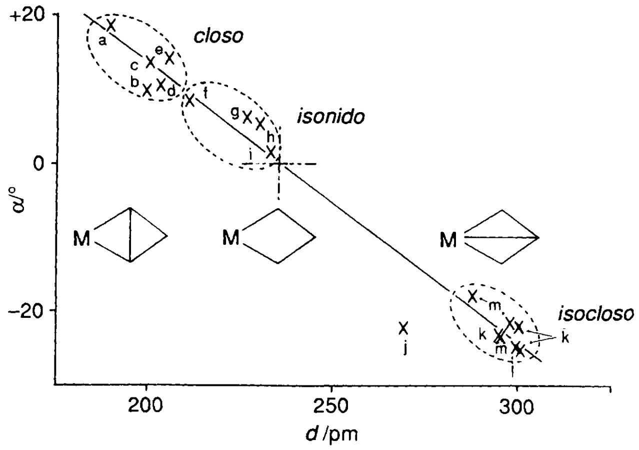

Fig. 7 A plot of the fold angle α between the Ir(7)–B(8)–B(9) and B(8)–B(9)–B(10) planes *versus* the B(8) ⋯ B(10) distance, *d*, for various *closo*, *isonido* and *isocloso* metallaboranes using values listed in Table 9 (numbering as in compounds **2**–**6**; structure **VIII**). Point j is for the carbaborane compound [$(PPh_3)(Ph_2PC_6H_4)IrB_8H_6(OMe)C(OH)$][6] **8** which contains a carbon atom in the open face of the cluster

this wide range of ten-vertex metallacarbaboranes and metallaborane clusters (or subclusters) *versus* the angle between the Ir(7)–B(8)–B(10) and B(8)–B(9)–B(10) planes (all numbered, for convenience, as for the *isonido* species, structure **VIII**). This figure demonstrates the continuum between the formally *closo* and formally *isocloso* cluster structures that passes through an *isonido* stage. The *closo* clusters may be regarded as opening up in the manner of a diamond(*closo*) ⟶ square(*isonido*) rearrangement on one face. Here it is of interest that many of the more classical *closo*-type species (points b, c, d, e in Fig. 7) already exhibit a lengthening of the B(8) ⋯ B(10) distance toward and beyond the 200 pm that may be taken as a weak bonding limit for interboron intracluster distances. In this manner, the available experimental examples constitute an essentially continuous geometric progression from *closo* to *isonido*. (Recently it has been recognised that this lengthening is also a general feature of *closo* ten-vertex heteroboranes where the hetero atom is not a metal one, and there are also indications of this type of behaviour in formally *closo* nine-vertex species too.[43]) The opening is followed by a square(*isonido*) ⟶ diamond(*isocloso*) closure, the overall *closo* ⟶ *isonido* ⟶ *isocloso* process necessitating a convex ⟶ concave change in the shape of the Ir(7)B(8)B(9)B(10) face (as the vertical scale in Fig. 7 passes through zero). Interestingly, compounds with clusters intermediate between the almost flat *isonido* 'square' and the concave *isocloso* 'diamond' have not yet been isolated. At present it is uncertain whether this merely reflects the type of systems that happen to have been investigated (in which case suitable examples might be discovered in future experiments) or whether it is a consequence of a 'catastrophic flip' from *isonido* to *isocloso* when the fold angle passes zero.

That this entire range of clusters lies close to the straight line in Fig. 7 suggests that there may be a systematic common bonding variation between the metal fragment and the borane fragment in this ten-vertex system. In this regard it is of interest that the open-face dimensions in the *isonido* compound **5**, with no bridging hydrogen atoms, are not particularly different to those of the hydrogen-bridged compounds **2** and **6**, even though it is slightly more displaced towards *isocloso* from *closo*. The smaller interplanar angle of +1.3(11)° in compound **5** may result from the absence of a bridging hydrogen atom, although the shortening of the Ir–B(8) distance by the chlorine substituent will also have an effect. {A similar but more marked shortening accounts[7] for the large 'concave' angle of the metallacarbaborane [$(PPh_3)(Ph_2PC_6H_4)IrB_8H_6(OMe)C(OH)$][6] **8** (point j in Fig. 7) which has a smaller carbon atom in the equivalent position.} In any event, examples from the continuum appear at present to fall into four categories, successively *closo*, hydrogen-bridged *isonido*, non-bridged *isonido*, and *isocloso*. Of these the known examples of the first three constitute a reasonably continuous progression, with as yet no examples between *isonido* and *isocloso*.

Cluster Electron-counting Considerations.—As discussed in the previous section the compounds described here form part of an interesting series of clusters which ranges from (*a*) the normal *closo* bicapped Archimedian-antiprism, through (*b*) the closely related group of *isonido* clusters, in which the dimensions have flexed to give a four-membered open face which then ultimately closes to give (*c*) the *isocloso* type of closed deltahedron (structures **I** ⟶ **V** ⟶ **IV** in Scheme 1). It is of particular interest that the two apparently different types of *isonido* compound, either with (compounds **2** and **6**) or without (**5**, **7** and **8**) bridging hydrogen atoms on the open face, together with variations such as the extra phosphine ligand on the cage (**7**) or a carbon atom (**8**) in the cluster, produce such similar structures.

Within the continuum the *isonido* clusters form a definitive cluster type with a square open face. As discussed in the Introduction, their geometries (structure **V**) can be derived from that of the *closo* eleven-vertex cluster by removal of a low-connectivity vertex (structure **VI**), rather than by removal of the high-connectivity vertex that would generate the conventional ten-vertex *nido* geometry (structure **III**). As such these *isonido* clusters are not in accord with the original cluster-geometry patterns initially delineated by Williams,[1] and consequently they are not accommodated by the electron-counting formalism initially put forward by Wade[2] to correlate these observed patterns of geometry with patterns of electronic constitution. There is therefore some interest in briefly discussing the constitution of these *isonido* species in this context.

The Williams–Wade formalism has been established for some time now.[1,2] It is summarised in many modern pregraduate general inorganic chemistry texts.[44] It offers a very useful basis from which to consider the ten-vertex *isonido* structure type.

In one approach to the electronic description of the *isonido* species it is convenient to consider first the ten-vertex conventionally[1,2] *closo* species [$1,2,2\text{-}(PPh_3)_3\text{-}2\text{-}H\text{-}closo\text{-}2,10\text{-}IrCB_8H_{10}$] **3** (Fig. 2),[24] and its relationship to the hydrogen-bridged *isonido* compound **2** with which it is formally isoelectronic. Compound **3** is a straightforward ten-vertex *closo* cluster compound in accord with the Williams–Wade[1,2] formalism. Thus it is a *closo*-$[B_{10}H_{10}]^{2-}$ analogue with ($2n$ + 2) cluster electrons, and in this analogy the {$IrH(PPh_3)_2$} unit contributes three orbitals and two electrons to the cluster bonding proper, *i.e.* it is a unit equivalent to {BH}, and it is an octahedral iridium(III) centre. Compared to **3**, the cluster of the *isonido* species **2** has one {HBH(bridge)} unit instead of the {CH} unit. On this basis **2** should be isoelectronic and therefore isostructural with **3**, *i.e.* *closo*, clearly at variance with its open nature. If this change from closed to open is associated with the gain of a cluster-electron pair, as it is for a conventional *closo* ⟶ *nido* opening,[1,2,45,46] then this electron pair would arise from the conversion of the non-cluster two-electron Ir–H terminal bond in compound **3** into the cluster Ir–H–B bridging bond in **2**. This would then engender a conventional[2] ($2n$ + 4) *nido* electron count for the open cluster of compound **2**, but thereby entail an unconventional four-orbital participation by the iridium centre in the cluster bonding proper [though still within the constraints of an eighteen-electron 'octahedral' iridium(III) configuration]. This removes it from Wade's original[2] three-orbital formalism, and at the same time generates a departure from Williams' original[1] geometric patterns because the metal atom thereby requires a high-connectivity open-face position.[3] It is unfortunate in this

Table 10 Data collection and structure solution and refinement parameters[a] for compounds **2**, **5** and **6**

	2	**5**	**6**
Formula	$C_{54}H_{55}B_9IrP_3$	$C_{54}H_{50}B_9ClIrP_3\cdot 3CH_2Cl_2$	$C_{54}H_{50.75}B_9Cl_{0.25}IrP_3\cdot 2CHCl_3$
M	1086.47	1371.68[b]	1329.81[b]
Crystal system	Monoclinic	Monoclinic	Triclinic
Space group	$P2_1/c$	$C2/c$	$P\bar{1}$
a/pm	1103.8(2)	4658.1(9)	1068.2(2)
b/pm	2990.4(7)	1393.3(3)	1353.6(3)
c/pm	1517.3(3)	1980.1(4)	2260.6(4)
α/°	—	—	93.16(2)
β/°	94.17(2)	93.98(2)	89.62(2)
γ/°	—	—	111.68(2)
U/nm^3	4.995(2)	12.323(4)	3.0326(11)
D_c/g cm^{-3}	1.44	1.49[b]	1.46[b]
Z	4	8	2
F(000)	2184	5306.6	1323.9
μ/cm^{-1}	26.77	24.60	24.68
No. of data collected	6563	5809	8470
No. observed[c]	5027	5582	8404
R[d]	0.0384	0.0780	0.0490
R'[e]	0.0397	0.0775	0.0518
Weighting factor g[f]	0.0008	0.0004	0.0006
No. of variables	526	564	571

[a] For compound **2**: scan width 2.0° + α-doublet splitting, scan speeds 2.0–29.3° min^{-1}. [b] Includes solvate molecules. [c] Criterion for observed reflections, $|F_o| > 4.0\sigma(|F_o|)$. [d] $\Sigma(|F_o| - |F_c|)/\Sigma|F_o|$. [e] $\Sigma w(|F_o| - |F_c|)^2/\Sigma w|F_o|^2$. [f] $w = [\sigma^2(|F_o|) + g(|F_o|)^2]^{-1}$.

context that a precise location of the two bridging hydrogen atoms in compound **2** has not been experimentally possible.

It is interesting that the *isonido* cluster geometry typified by compound **2** is not substantially altered when two electrons are removed from this compound type by the notional removal of two hydrogen atoms to generate compound **5**. This suggests that, if the electronic requirements of this cluster shape are essentially unchanged from **2** to **5**, then the two additional electrons would now have to come from the iridium centre which would then have to be described as sixteen-electron iridium(v). Again, as with the eighteen-electron iridium(III) centre as in **2**, this would imply a four-orbital contribution by the iridium centre to the cluster bonding to generate a $(2n + 4)$ *nido* cluster-electron count.

These two variants of a four-orbital approach are consistent with a very similar four-orbital approach that has been used to account for the ten-vertex '*isocloso*' structures.[4,13,47] These last also adopt a shape (structure **IV**) not originally listed by Williams,[1] but which nevertheless is a closed deltahedron, and for these structures a four-orbital metal contribution would have to be invoked to engender a conventional[2] *closo* $(2n + 2)$ electron count. Here, however, it should be mentioned that an alternative $2n$-electron '*hypercloso*' three-orbital approach to the *isocloso* geometry **IV** has also been proposed[11,12,14] and the four-orbital approach thereby very strongly questioned,[14] but it is not clear at present how this *hypercloso* approach could be extended to a $(2n + 2)$-electron '*hypernido*' description of the *isonido* structures we describe. It would be instructive to see rigorous molecular orbital calculations in this general area (see also discussion in ref. 48, pp. 223–225).

Mechanistic Considerations.—The initial formation of compound **2** from the *nido*-$[B_9H_{12}]^-$ anion and $[IrCl(PPh_3)_3]$ may be regarded stoichiometrically as occurring *via* a simple metathesis together with a transfer of the phosphine to the cluster and loss of dihydrogen [equation (4)]. A more detailed mechanism is more difficult to piece together. The phosphine

$$[NEt_4][B_9H_{12}] + [IrCl(PPh_3)_3] \longrightarrow [(PPh_3)_2IrB_9H_{10}(PPh_3)] + NEt_4Cl + H_2 \quad (4)$$

addition may well occur *via* intracluster migration since experiments in which an excess of PPh_3 is added to the reaction mixture before addition of the $[B_9H_{12}]^-$ anion do not show any marked increase in products with a phosphine substituent. The open face in the product implies a break in a direct B–B linkage of the borane anion during the course of the reaction. The production of *isonido*-iridadecaborane compounds from the thermolysis of a *nido* precursor to produce compounds **5** and **6** (see following paragraph) introduces the possibility that, in the $[B_9H_{12}]^-$ reaction shown in equation (4), compound **2** could result from a phosphine-substituted intermediate of formulation such as $\{(PPh_3)_2IrB_9H_{12}(PPh_3)\}$. This latter could in principle be *nido* or *isonido* and could therefore be the intermediate that undergoes the crucial *nido* $\longrightarrow$ *isonido* closure, either before or associated with the loss of dihydrogen to give compound **2**. That compound **2** is also a product of the reaction of $[IrCl(PPh_3)_3]$ and the *arachno*-$[B_9H_{14}]^-$ anion suggests that this type of intermediate could also be accessible *via* the loss of two hydrogen atoms from a 'higher' intermediate of a $\{(PPh_3)_2HIrB_9H_{13}(PPh_3)\}$ type of formulation. In this context the absence of an *o*-cycloboronated phosphine ligand in compound **2** should be mentioned since it has been suggested[4] that, in some reaction pathways within this type of system, *o*-cycloboronation occurs in order to provide electrons for the formation of the stable conventionally shaped *nido*-decaborane type cluster **VI**. The absence of *o*-cycloboronation in compound **2** itself is not unexpected, however, since in this case both starting nonaborane anions contain an excess of electrons (as hydrogen atoms) over those required both to form this particular product and to form reasonably postulated intermediates that would lead to it.

The general mechanism for the formation of compounds **5** and **6** is, in one respect, somewhat less speculative in that the structure of the *nido*-5-iridadecaborane compound **4** from which they are derived is well established.[8] Their formation from the *nido*-5-iridadecaborane cluster is of particular interest as it has been suggested[4,8] that *isonido*-type clusters are in fact intermediates in certain *nido*-iridadecaborane reaction sequences such as (*a*) the formation of *isocloso*-iridadecaboranes *via* the thermolysis of *nido*-5 and *nido*-6-iridadecaboranes,[4] and (*b*) the isomerisation of *nido*-6-iridadecaborane clusters to *nido*-5-iridadecaboranes.[8] This work now shows that *isonido* clusters can indeed be formed from a *nido*-5-iridadecaborane cluster, albeit one (compound **4**) containing a phosphine substituent. Two routes to the observed *isonido* products can be postulated.

(*a*) *via* a vertex-swing of the B(6) vertex of the *nido*-5-

Table 11 Atom coordinates (× 10^4) for compound **2** with e.s.d.s in parentheses

Atom	*x*	*y*	*z*	Atom	*x*	*y*	*z*
Ir(7)	2040.4(2)	1532.5(1)	3673.3(1)	C(222)	1871(4)	1805(2)	6435(3)
P(1)	2891(2)	2251(1)	3874(1)	C(223)	2059(4)	2122(2)	7106(3)
P(2)	2622(2)	1243(1)	5075(1)	C(224)	3222(4)	2290(2)	7319(3)
P(3)	2900(2)	540(1)	1161(1)	C(225)	4197(4)	2142(2)	6861(3)
B(1)	−259(9)	1294(4)	2386(7)	C(226)	4009(4)	1825(2)	6190(3)
B(2)	488(8)	1006(4)	3321(6)	C(231)	4048(4)	915(2)	5245(3)
B(3)	90(9)	1587(4)	3296(7)	C(232)	4479(4)	805(2)	6104(3)
B(4)	904(9)	1728(4)	2366(7)	C(233)	5536(4)	552(2)	6249(3)
B(5)	848(9)	1269(3)	1571(6)	C(234)	6162(4)	409(2)	5534(3)
B(6)	563(8)	777(3)	2241(7)	C(235)	5731(4)	519(2)	4675(3)
B(8)	2227(8)	1421(3)	2176(6)	C(236)	4674(4)	772(2)	4530(3)
B(9)	1949(8)	901(3)	1871(6)	C(311)	2349(6)	−26(2)	998(4)
B(10)	1929(8)	848(3)	2975(6)	C(312)	1981(6)	−256(2)	1732(4)
C(111)	4542(3)	2292(2)	4160(3)	C(313)	1597(6)	−700(2)	1647(4)
C(112)	5270(5)	1912(2)	4131(3)	C(314)	1582(6)	−913(2)	829(4)
C(113)	6529(3)	1949(2)	4273(3)	C(315)	1950(6)	−682(2)	95(4)
C(114)	7059(3)	2366(2)	4443(3)	C(316)	2334(6)	−239(2)	179(4)
C(115)	6331(3)	2747(2)	4472(3)	C(321)	3020(6)	772(2)	73(3)
C(116)	5072(3)	2710(2)	4330(3)	C(322)	4145(6)	886(2)	−226(3)
C(121)	2857(5)	2626(2)	2907(3)	C(323)	4207(6)	1079(2)	−1059(3)
C(122)	2177(5)	3020(2)	2854(3)	C(324)	3145(6)	1158(2)	−1592(3)
C(123)	2239(5)	3302(2)	2127(3)	C(325)	2020(6)	1044(2)	−1292(3)
C(124)	2980(5)	3191(2)	1453(3)	C(326)	1958(6)	851(2)	−460(3)
C(125)	3659(5)	2798(2)	1506(3)	C(331)	4445(4)	488(2)	1655(3)
C(126)	3598(5)	2515(2)	2233(3)	C(332)	4990(4)	862(2)	2063(3)
C(131)	2113(5)	2592(2)	4672(3)	C(333)	6206(4)	846(2)	2385(3)
C(132)	861(5)	2637(2)	4495(3)	C(334)	6876(4)	455(2)	2299(3)
C(133)	202(5)	2918(2)	5017(3)	C(335)	6331(4)	80(2)	1891(3)
C(134)	794(5)	3153(2)	5716(3)	C(336)	5115(4)	97(2)	1569(3)
C(135)	2046(5)	3108(2)	5892(3)	H(1)	−1079(61)	1315(22)	2214(41)
C(136)	2706(5)	2827(2)	5370(3)	H(2)	124(46)	826(18)	3874(35)
C(211)	1482(4)	856(2)	5477(3)	H(3)	−490(64)	1782(21)	3752(54)
C(212)	291(4)	1006(2)	5521(3)	H(4)	785(76)	2045(31)	2267(54)
C(213)	−583(4)	723(2)	5839(3)	H(5)	426(56)	1384(21)	905(41)
C(214)	−265(4)	290(2)	6112(3)	H(6)	252(64)	461(26)	1961(45)
C(215)	926(4)	141(2)	6068(3)	H(8)	2905(76)	1619(26)	1907(54)
C(216)	1800(4)	424(2)	5751(3)	H(10)	2406(49)	571(20)	3266(35)
C(221)	2846(4)	1657(2)	5977(3)				

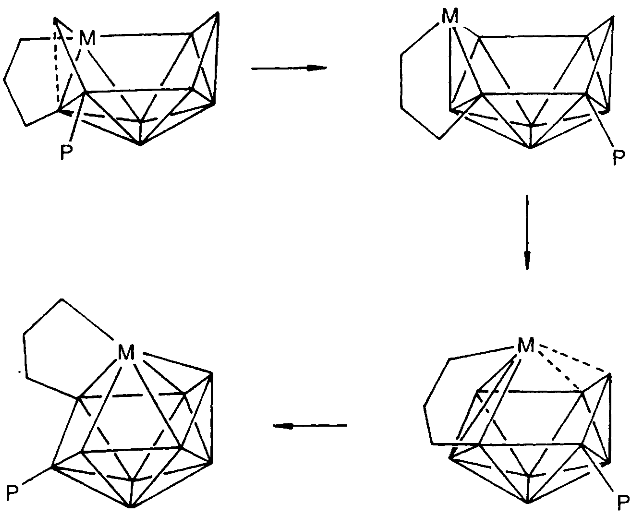

Scheme 2

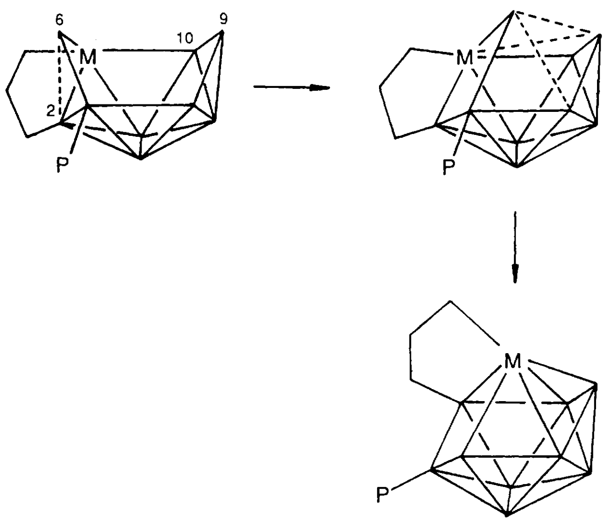

Scheme 3

iridadecaborane cluster in compound **4** to give a *nido*-6-iridadecaborane intermediate (Scheme 2), this being an effective reversal of the geometry of one of the possible steps in the formation of compound **4**.[8,9] The intermediate cluster would then close up to give an *isonido* product with *ortho*-phenylation to a boron vertex in the open face. However, although examples of *nido*-6-metalladecaborane clusters which directly undergo a 6 to 5 change in the site of the metal are known[9,49] the reverse as far as we are aware has yet to be observed.

(*b*) *via* a direct closure of the *nido*-5-iridadecaborane cluster that would involve a break in the B(6)–B(2) connection (Scheme 3). It may be noted that movement of B(6) towards

Table 12 Atom coordinates (× 10^4) for compound **5** with e.s.d.s in parentheses

Atom	*x*	*y*	*z*	Atom	*x*	*y*	*z*
Ir(7)	1366.2(2)	544.8(5)	−1190.4(3)	C(213)	1144(3)	−1977(9)	827(5)
P(1)	1842(1)	171(4)	−751(2)	C(214)	1388(3)	−2578(9)	925(5)
P(2)	1172(1)	−1063(4)	−1144(2)	C(215)	1561(3)	−2754(9)	390(5)
P(3)	586(1)	2595(3)	−357(2)	C(216)	1490(3)	−2329(9)	−243(5)
Cl(8)	1377(1)	2180(4)	151(2)	C(221)	782(2)	−922(9)	−1199(6)
B(1)	1185(5)	2375(14)	−2123(11)	C(222)	672(2)	39(9)	−1303(6)
B(2)	1046(5)	1070(18)	−2132(9)	C(223)	377(2)	179(9)	−1443(6)
B(3)	1434(4)	1418(17)	−2078(10)	C(224)	193(2)	−642(9)	−1479(6)
B(4)	1458(5)	2262(18)	−1350(10)	C(225)	303(2)	−1603(9)	−1374(6)
B(5)	1120(5)	2865(14)	−1319(10)	C(226)	598(2)	−1742(9)	−1234(6)
B(6)	847(5)	2116(17)	−1806(11)	C(231)	1233(3)	−1931(9)	−1824(6)
B(8)	1224(5)	1961(14)	−760(12)	C(232)	1279(3)	−1545(9)	−2463(6)
B(9)	869(4)	2091(15)	−928(9)	C(233)	1319(3)	−2189(9)	−3001(6)
B(10)	881(5)	935(19)	−1322(13)	C(234)	1315(3)	−3220(9)	−2902(6)
C(111)	2116(2)	1059(8)	−974(6)	C(235)	1269(3)	−3606(9)	−2264(6)
C(112)	2316(2)	823(8)	−1440(6)	C(236)	1229(3)	−2962(9)	−1725(6)
C(113)	2528(2)	1514(8)	−1585(6)	C(311)	610(3)	3922(8)	−206(7)
C(114)	2538(2)	2441(8)	−1263(6)	C(312)	375(3)	4556(8)	−336(7)
C(115)	2337(2)	2677(8)	−797(6)	C(313)	402(3)	5575(8)	−200(7)
C(116)	2126(2)	1986(8)	−652(6)	C(314)	664(3)	5960(8)	67(7)
C(121)	1916(3)	93(9)	166(4)	C(315)	899(3)	5326(8)	197(7)
C(122)	1688(3)	−51(9)	575(4)	C(316)	872(3)	4307(8)	60(7)
C(123)	1742(3)	−196(9)	1270(4)	C(321)	219(2)	2351(10)	−679(6)
C(124)	2024(3)	−197(9)	1555(4)	C(322)	123(2)	2716(10)	−1315(6)
C(125)	2252(3)	−53(9)	1146(4)	C(323)	−150(2)	2462(10)	−1595(6)
C(126)	2198(3)	92(9)	451(4)	C(324)	−327(2)	1842(10)	−1239(6)
C(131)	1977(3)	−986(8)	−1084(6)	C(325)	−231(2)	1477(10)	−603(6)
C(132)	1914(3)	−1215(8)	−1766(6)	C(326)	42(2)	1731(10)	−324(6)
C(133)	2017(3)	−2099(8)	−2034(6)	C(331)	617(3)	2037(9)	487(5)
C(134)	2182(3)	−2754(8)	−1620(6)	C(332)	731(3)	1078(9)	569(5)
C(135)	2245(3)	−2526(8)	−938(6)	C(333)	734(3)	608(9)	1198(5)
C(136)	2142(3)	−1642(8)	−671(6)	C(334)	624(3)	1097(9)	1745(5)
C(211)	1246(3)	−1728(9)	−341(5)	C(335)	510(3)	2056(9)	1663(5)
C(212)	1073(4)	−1552(9)	194(5)	C(336)	507(3)	2526(9)	1033(5)

Ir(5)–B(9)–B(10), *i.e.* in the opposite direction to that shown in Scheme 3, would in principle result in a *closo*-type cluster with the metal vertex in the apical B(1) position (numbered as in $[B_{10}H_{10}]^{2-}$), and not an *isonido* cluster (compare and contrast ref. 30).

Clearly, there are elements of uncertainty in these proposed mechanisms for the formation of these low-yield compounds, but conversely it seems reasonable that these *isonido* types of cluster may also be transition states or intermediates in many of the vertex-swing processes that seem to occur[9,10] in a wide range of ten-vertex metallaborane, metallacarbaborane and carbaborane clusters.

Experimental

General.—The compounds $[IrCl(PPh_3)_3]$, $[NEt_4][$*nido*-$B_9H_{12}]$, $[NEt_4][$*arachno*-$B_9H_{14}]$ and the *nido*-iridadecaborane $[5,7\text{-}(PPh_3)_2\text{-}5\text{-}H\text{-}5\text{-}(o\text{-}Ph_2PC_6H_4)$-*nido*-$5\text{-}IrB_9H_{10}\text{-}2]$ were prepared as described previously.[8] Reactions were carried out under a dry nitrogen atmosphere although separatory procedures were carried out in air. Preparative and analytical thin-layer chromatography (TLC) were performed using silica gel (with a fluorescent indicator; Fluka type GF-254) as stationary phase, with general techniques as described in previous papers from our laboratories.[4,8,9] Infrared spectra were recorded from KBr discs using a Perkin-Elmer 457 grating spectrometer.

NMR Spectroscopy.—Lower-field ^1H (*ca.* 100 MHz), ^{31}P (*ca.* 40 MHz) and ^{11}B (*ca.* 32 MHz) NMR data were obtained using a pulse-FT JEOL FX100 instrument. $^{31}P\text{-}\{^1H$(broad-band noise)$\}$ spectra were recorded at lower temperatures to maximise line sharpening arising from the 'thermal decoupling' of the effects of boron nuclear spins.[27,28] Higher-field (128 MHz) ^{11}B and $^{11}B\text{-}\{^1H\}$ experiments were carried out on a Bruker WH-400 pulse FT spectrometer as part of the SERC service at Sheffield University. Some selective $^1H\text{-}\{^{11}B\}$ NMR experiments were also carried out on a Bruker WH-360 pulse-FT instrument as part of the SERC service at the University of Edinburgh. Chemical shifts δ are given in ppm to high frequency (low field) of Ξ100 MHz ($SiMe_4$) for ^1H (quoted ± 0.05 ppm), of Ξ32.083 971 MHz [nominally $BF_3(OEt_2)$ in $CDCl_3$] for ^{11}B (quoted ±0.5 ppm), and of Ξ40.480 730 MHz (nominally 85% H_3PO_4) for ^{31}P (quoted ±0.5 ppm), Ξ being defined as in ref. 50. Spectra were calibrated for δ using solvent resonances as internal secondary standards.

Isolation of $[7,7,9\text{-}(PPh_3)_3$-*isonido*-$7\text{-}IrB_9H_{10}]$ **2**.—The salt $[NEt_4][$*nido*-$B_9H_{12}]$ (0.04 g, 0.15 mmol) was added to a stirred solution of $[IrCl(PPh_3)_3]$ (0.15 g, 0.15 mmol) in dichloromethane (*ca.* 30 cm^3). The mixture was stirred for 45 min, then reduced in volume on a rotary evaporator (room temperature, water-pump pressure) to *ca.* 2 cm^3, and applied to a preparative TLC plate. The plate was developed using CH_2Cl_2–pentane (1:1) as the mobile phase. A number of yellow bands were apparent with $R_f > 0.5$, of which the isolation and characterisation (as a variety of *nido*-iridadecaborane cluster compounds) has been described elsewhere.[8] A further pale violet band (R_f 0.2, 3 mg, 2% yield) was isolated, and characterised after repeated TLC purification as $[7,7,9\text{-}(PPh_3)_3$-*isonido*-$7\text{-}IrB_9H_{10}]$ **2** as described in the text. Compound **2** was similarly isolated in a similar yield from the otherwise analogous reaction of $[NEt_4][$*arachno*-$B_9H_{14}]$ with $[IrCl(PPh_3)_3]$, as described previously.[7,8] In this case the major product was the *nido*-6-iridadecaborane $[H(PPh_3)_2IrB_9H_{13}]$[8,18] **1** in 81% yield. No

Table 13 Atom coordinates (× 10^4) for compound **6** with e.s.d.s in parentheses

Atom	*x*	*y*	*z*
Ir(7)	3104.6(3)	396.6(2)	2256.2(1)
P(1)	2115(2)	234(2)	1316(1)
P(2)	2796(2)	1871(2)	2652(1)
P(3)	1328(2)	−2193(2)	3817(1)
B(1)	5148(9)	−672(7)	2680(4)
B(2)	4817(8)	521(7)	2940(4)
B(3)	5034(9)	182(8)	2170(5)
B(4)	3745(8)	−1116(6)	2122(4)
B(5)	3603(8)	−1769(7)	2830(4)
B(6)	4300(8)	−657(7)	3374(4)
B(8)	2269(8)	−1358(6)	2562(4)
B(9)	2594(8)	−1321(6)	3289(4)
B(10)	3162(8)	28(7)	3234(4)
C(111)	2338(5)	−731(3)	764(2)
C(112)	3650(5)	−669(3)	653(2)
C(113)	3886(5)	−1340(3)	213(2)
C(114)	2810(5)	−2073(3)	−116(2)
C(115)	1498(5)	−2135(3)	−5(2)
C(116)	1262(5)	−1464(3)	435(2)
C(121)	266(4)	−157(3)	1333(2)
C(122)	−428(4)	393(3)	1061(2)
C(123)	−1828(4)	41(3)	1096(2)
C(124)	−2534(4)	−861(3)	1403(2)
C(125)	−1839(4)	−1410(3)	1675(2)
C(126)	−439(4)	−1058(3)	1640(2)
C(131)	2758(4)	1399(3)	882(2)
C(132)	3793(4)	2308(3)	1115(2)
C(133)	4327(4)	3198(3)	779(2)
C(134)	3826(4)	3180(3)	208(2)
C(135)	2791(4)	2272(3)	−26(2)
C(136)	2256(4)	1381(3)	311(2)
C(211)	1273(4)	2084(3)	2419(2)
C(212)	1296(4)	2745(3)	1963(2)
C(213)	106(4)	2843(3)	1778(2)
C(214)	−1108(4)	2279(3)	2048(2)
C(215)	−1131(4)	1617(3)	2503(2)
C(216)	59(4)	1520(3)	2689(2)
C(221)	4160(5)	3184(3)	2614(2)
C(222)	3923(5)	4127(3)	2708(2)
C(223)	4993(5)	5106(3)	2706(2)
C(224)	6301(5)	5143(3)	2610(2)
C(225)	6538(5)	4201(3)	2516(2)
C(226)	5468(5)	3221(3)	2518(2)
C(231)	2605(4)	1711(3)	3440(2)
C(232)	2825(4)	856(3)	3673(2)
C(233)	2807(4)	759(3)	4285(2)
C(234)	2568(4)	1518(3)	4663(2)
C(235)	2348(4)	2374(3)	4430(2)
C(236)	2366(4)	2470(3)	3819(2)
C(311)	1752(4)	−1845(3)	4589(2)
C(312)	893(4)	−1566(3)	4973(2)
C(313)	1278(4)	−1254(3)	5564(2)
C(314)	2522(4)	−1220(3)	5770(2)
C(315)	3381(4)	−1499(3)	5836(2)
C(316)	2996(4)	−1811(3)	4796(2)
C(321)	−329(4)	−2124(3)	3708(2)
C(322)	−1476(4)	−2921(3)	3911(2)
C(323)	−2741(4)	−2865(3)	3832(2)
C(324)	−2860(4)	−2011(3)	3551(2)
C(325)	−1713(4)	−1214(3)	3349(2)
C(326)	−447(4)	−1270(3)	3427(2)
C(331)	1028(4)	−3596(3)	3709(2)
C(332)	905(4)	−4236(6)	4186(2)
C(333)	541(4)	−5334(3)	4086(2)
C(334)	300(4)	−5791(3)	3509(2)
C(335)	424(4)	−5151(3)	3032(2)
C(336)	788(4)	−4054(3)	3132(2)
H(1)	6286(19)	−782(19)	2739(18)
H(2)	5472(19)	1133(18)	3115(17)
H(4)	3597(19)	−1684(19)	1634(18)
H(5)	3598(19)	−2653(18)	2838(16)
H(6)	4913(18)	−603(18)	3748(16)
H(8)	1279(19)	−1893(18)	2284(16)

70 eV electron impact (EI) mass spectrum was obtainable for **2**, as is often the case in these polyphosphine-substituted iridaborane clusters of high molecular weight. Some relevant infrared data are listed in Table 4. In addition, compound **2** features a strong band at 2500 cm^{-1} due to B–H stretching. Mauve crystals of **2** suitable for X-ray diffraction analysis were obtained by diffusion of pentane into a solution of the compound in dichloromethane.

Isolation of Compounds [8-Cl-7,9-(PPh$_3$)$_2$-7-(*o*-Ph$_2$P-C$_6$H$_4$)-*isonido*-7-IrB$_9$H$_6$-10] **5** *and* [7,9-(PPh$_3$)$_2$-7-(*o*-Ph$_2$PC$_6$H$_4$)-*isonido*-7-IrB$_9$H$_9$-10] **6**.—A solution of [5,7-(PPh$_3$)$_2$-5-H-5-(*o*-Ph$_2$PC$_6$H$_4$)-*nido*-5-IrB$_9$H$_{10}$-2] **4** (200 mg, 0.2 mmol) in 1,1,2,2-tetrachloroethane (2 cm^3) was heated at *ca.* 70 °C for 1 h. The resultant mixture was chromatographed by TLC using CH$_2$Cl$_2$–pentane (80:20) as the mobile phase. A number of coloured bands were evident. The first, a red band (R_f 0.7, 10 mg), has similar features in its multielement NMR spectra to the *isonido* compounds reported here, but it has not yet been fully characterised. The second, a deep purple band (R_f 0.65, 10 mg, 5% yield) was characterised after repeated TLC purification as [8-Cl-7,9-(PPh$_3$)$_2$-7-(*o*-Ph$_2$PC$_6$H$_4$)-*isonido*-7-IrB$_9$H$_6$-10] **5** as described in the text. The third, a royal-blue band (R_f 0.6, 3 mg, 1.5% yield), was similarly isolated and purified, and characterised as [7,9-(PPh$_3$)$_2$-7-(*o*-Ph$_2$PC$_6$H$_4$)-*isonido*-7-IrB$_9$H$_9$-10] **6** as described in the text. As with compound **2**, no 70 eV EI mass spectra were obtainable for **5** or **6**. Crystals of compound **5** suitable for X-ray diffraction analysis were obtained by diffusion of pentane into a dichloromethane solution of the compound, and of **6** by diffusion of pentane into a chloroform solution.

X-Ray Diffraction Analysis.—Crystallographic measurements for compound **2** were made on a Syntex $P2_1$ diffractometer operating in the ω–2θ scan mode using graphite-monochromated Mo-Kα radiation (λ = 71.069 pm) following a procedure described elsewhere in detail.[51] Crystallographic measurements for compounds **5** and **6** were made on a Philips PW1000 diffractometer using Mo-Kα radiation from a graphite monochromator and operating in the θ-2θ scan mode using a technique previously described.[52]

The structures were solved *via* standard heavy-atom procedures and were refined by full-matrix least squares using the SHELX program system.[53] All three data sets were corrected for absorption empirically once the structures had been determined.[54] Refinement of all three structures was basically the same with all non-hydrogen atoms assigned anisotropic thermal parameters, except for those of three disordered CH$_2$Cl$_2$ solvent molecules of compound **5** and those of two disordered CHCl$_3$ solvent molecules of compound **6**, which were refined with isotropic thermal parameters. For compound **6** a large peak was located in the Fourier difference map at *ca.* 180 pm from the B(3) atom; this was treated as a chlorine atom of partial occupancy 0.25 and was refined with an isotropic thermal parameter. All phenyl groups were included in the refinement as rigid bodies with hexagonal symmetry (C–C 139.5 pm). All phenyl hydrogen atoms were included in calculated positions (C–H 96 pm) and refined with an overall isotropic thermal parameter. All the borane hydrogen atoms in compounds **2** and **6** were located (except for those bridging hydrogen atoms associated with the open faces, see discussion in text) and were refined freely with individual isotropic thermal parameters. Borane hydrogen atoms were not located for compound **5**.

Details of the crystal data, data collection and structure refinement parameters are given in Table 10 and atomic coordinates for compounds **2**, **5** and **6** are in Tables 11, 12 and 13 respectively.

Additional material available from the Cambridge Crystallographic Data Centre comprises remaining H-atom coordinates, thermal parameters and remaining bond lengths and angles.

Acknowledgements

We thank Drs. B. E. Mann, C. Spencer and D. Reed for high-field NMR spectra obtained as part of the SERC service at Sheffield and Edinburgh Universities, Dr. B. Štíbr for interesting discussions,[43] and Professor N. N. Greenwood for his interest in some of the early stages of this work.[16] We also thank Drs. J. E. Crook and W. S. McDonald for assistance and advice in some of the early stages of some of the crystallography.

References

1 R. E. Williams, *Inorg. Chem.*, 1971, **10**, 210; *Adv. Inorg. Chem. Radiochem.*, 1976, **18**, 67.
2 K. Wade, *Chem. Commun.*, 1971, 792; *Adv. Inorg. Chem. Radiochem.*, 1976, **18**, 1.
3 R. E. Williams, in *Electron Deficient Boron and Carbon Clusters*, eds. G. A. Olah, K. Wade and R. E. Williams, Wiley-Interscience, New York and Chichester, 1991, ch. 2, pp. 11–93.
4 J. Bould, N. N. Greenwood, J. D. Kennedy and W. S. McDonald, *J. Chem. Soc., Chem. Commun.*, 1982, 465; J. Bould, N. N. Greenwood and J. D. Kennedy, *J. Chem. Soc., Dalton Trans.*, 1990, 1451.
5 J. D. Kennedy, *Prog. Inorg. Chem.*, 1986, **34**, 211.
6 J. E. Crook, N. N. Greenwood, J. D. Kennedy and W. S. McDonald, *J. Chem. Soc., Chem. Commun.*, 1981, 933.
7 J. Bould, P. Brint, J. D. Kennedy and M. Thornton-Pett, *Acta Crystallogr., Sect. C*, 1990, **46**, 1010.
8 J. Bould, N. N. Greenwood and J. D. Kennedy, *J. Chem. Soc., Dalton Trans.*, 1990, 1441.
9 J. Bould, J. E. Crook, J. D. Kennedy and M. Thornton-Pett, unpublished work.
10 See, for example, M. Bown, T. Jelínek, B. Štíbr, S. Heřmánek, X. L. R. Fontaine, N. N. Greenwood, J. D. Kennedy and M. Thornton-Pett, *J. Chem. Soc., Chem. Commun.*, 1988, 1972, and refs. therein.
11 R. T. Baker, *ACS Symp. Ser.*, 1983, **211**, 346.
12 R. T. Baker, *Inorg. Chem.*, 1986, **25**, 109.
13 J. D. Kennedy, *Inorg. Chem.*, 1986, **25**, 111.
14 R. D. Johnston and D. M. P. Mingos, *Inorg. Chem.*, 1986, **25**, 3321.
15 J. Bould, Ph.D. Thesis, University of Leeds, 1983.
16 N. N. Greenwood and J. D. Kennedy, in *Metal Interactions with Borane Clusters*, ed. R. N. Grimes, Plenum, New York, 1982, ch. 2.
17 N. N. Greenwood, *ACS Symp. Ser.*, 1983, **232**, 125.
18 J. Bould, N. N. Greenwood, J. D. Kennedy and W. S. McDonald, *J. Chem. Soc., Dalton Trans.*, 1982, 713.
19 J. E. Crook, Ph.D. Thesis, University of Leeds, 1983.
20 J. L. Bookham, X. L. R. Fontaine, J. D. Kennedy and W. McFarlane, *Inorg. Chem.*, 1987, **28**, 1111: see also, for example, J. D. Kennedy, W. McFarlane and D. S. Rycroft, *Inorg. Chem.*, 1973, **12**, 2742, and refs. therein.
21 N. N. Greenwood, J. D. Kennedy, M. Thornton-Pett and J. D. Woollins, *J. Chem. Soc., Dalton Trans.*, 1985, 2397.
22 X. L. R. Fontaine, H. Fowkes, N. N. Greenwood, J. D. Kennedy and M. Thornton-Pett, *J. Chem. Soc., Dalton Trans.*, 1987, 2417.
23 J. Bould, N. N. Greenwood and J. D. Kennedy, *J. Chem. Soc., Dalton Trans.*, 1982, 481.
24 S. K. Boocock, N. N. Greenwood, J. D. Kennedy, W. S. McDonald and J. Staves, *J. Chem. Soc., Dalton Trans.*, 1981, 2573.
25 M. McGrath, T. R. Spalding, X. L. R. Fontaine, J. D. Kennedy and M. Thornton-Pett, *J. Chem. Soc., Dalton Trans.*, 1991, 3223, and refs. therein.
26 J. D. Kennedy, B. Štíbr, M. Thornton-Pett and T. Jelínek, *Inorg. Chem.*, 1991, **30**, 4481; see also J. D. Kennedy, B. Štíbr, T. Jelínek, X. L. R. Fontaine and M. Thornton-Pett, *Collect. Czech. Chem. Commun.*, submitted.
27 H. Beall, A. T. Elvin and C. Bushweller, *Inorg. Chem.*, 1974, **13**, 2031.
28 J. D. Kennedy and J. Staves, *Z. Naturforsch., Teil B*, 1979, **34**, 808.
29 J. Bould, J. E. Crook, N. N. Greenwood and J. D. Kennedy, *J. Chem. Soc., Dalton Trans.*, 1984, 1903.
30 N. W. Alcock, J. G. Taylor and M. G. H. Wallbridge, *J. Chem. Soc., Chem. Commun.*, 1983, 1168.
31 K. Nestor, X. L. R. Fontaine, N. N. Greenwood, J. D. Kennedy, J. Plešek, B. Štíbr and M. Thornton-Pett, *Inorg. Chem.*, 1989, **28**, 2219.
32 A. G. Orpen, HYDEX and XHYDEX, programs for the indirect location of hydrogen atoms using potential-well calculations.
33 M. Thornton-Pett, A. G. Orpen and J. D. Kennedy, unpublished work.
34 M. A. Beckett, N. N. Greenwood, J. D. Kennedy and M. Thornton-Pett, *J. Chem. Soc., Dalton Trans.*, 1986, 795.
35 M. A. Beckett, N. N. Greenwood, J. D. Kennedy and M. Thornton-Pett, *J. Chem. Soc., Dalton Trans.*, 1985, 1119.
36 J. D. Kennedy, in *Boron Chemistry* (*IMEBORON 6*), ed. S. Heřmánek, World Scientific, Singapore, 1987, pp. 207–243.
37 J. R. Pipal and R. N. Grimes, *Inorg. Chem.*, 1979, **18**, 257.
38 J. Bould, P. Brint, X. L. R. Fontaine, J. D. Kennedy and M. Thornton-Pett, *J. Chem. Soc., Chem. Commun.*, 1989, 1763; also unpublished work.
39 J. E. Crook, M. Elrington, N. N. Greenwood, J. D. Kennedy, M. Thornton-Pett and J. D. Woollins, *J. Chem. Soc., Dalton Trans.*, 1985, 2407.
40 K. Nestor, Ph.D. Thesis, University of Leeds, 1989.
41 X. L. R. Fontaine, H. Fowkes, N. N. Greenwood, J. D. Kennedy and M. Thornton-Pett, *J. Chem. Soc., Dalton Trans.*, 1987, 1431.
42 E. J. Ditzel, X. L. R. Fontaine, N. N. Greenwood, J. D. Kennedy and M. Thornton-Pett, *J. Chem. Soc., Chem Commun.*, 1989, 1262.
43 K. Nestor, J. D. Kennedy, B. Štíbr and M. Thornton-Pett, *Collect. Czech. Chem. Commun.*, in the press; B. Štíbr, J. D. Kennedy, M. Thornton-Pett, E. Drdáková, T. Jelínek and J. Plešek, *Collect. Czech. Chem. Commun.*, in the press.
44 See, for example, F. A. Cotton and G. Wilkinson, *Inorganic Chemistry*, 4th edn., Wiley, New York, 1980; 5th edn., Wiley, New York, 1988; J. E. Huheey, *Inorganic Chemistry*, 3rd edn., Harper Collins, New York, 1983; N. N. Greenwood and A. Earnshaw, *The Chemistry of the Elements*, Pergamon, Oxford, 1984; D. F. S. Shriver, P. W. Atkins and C. H. Landford, *Inorganic Chemistry*, Oxford University Press, Oxford, 1990; S. M. Owen and A. T. Brooker, *A Guide to Modern Inorganic Chemistry*, Longman, Harlow, 1991.
45 R. W. Rudolph and W. R. Pretzer, *Inorg. Chem.*, 1972, **11**, 1974.
46 R. W. Rudolph, *Accounts Chem. Res.*, 1976, **9**, 446.
47 H. Fowkes, N. N. Greenwood, J. D. Kennedy and M. Thornton-Pett, *J. Chem. Soc., Dalton Trans.*, 1986, 517.
48 A. A. Aradi and T. P. Fehlner, *Adv. Organomet. Chem.*, 1990, **30**, 189.
49 D. F. Gaines, J. W. Lott and J. C. Calabrese, *Inorg. Chem.*, 1974, **13**, 2419.
50 W. McFarlane, *Proc. R. Soc. London, Ser. A.*, 1968, **306**, 185.
51 A. Modinos and P. Woodward, *J. Chem. Soc., Dalton Trans.*, 1974, 2065.
52 K. R. Adams, G. Anderegg, L. F. Lindoy, H. C. Lip, M. McPartlin, J. H. Rea, R. J. Smith and P. A. Tasker, *Inorg. Chem.*, 1980, **19**, 2956.
53 G. M. Sheldrick, SHELX 76, Program System for X-Ray Structure Determination, University of Cambridge, 1976.
54 N. Walker and D. Stuart, *Acta Crystallogr., Sect. A*, 1983, **39**, 158.

Received 30*th July* 1991; *Paper* 1/03934B